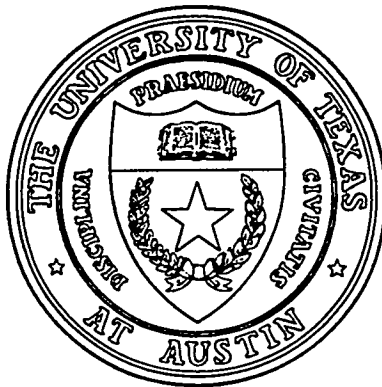


UTEXAS-HEP-95-18

DOE/ER/40757-074

CONF-9507201-2



SEARCHES FOR VERY RARE DECAYS OF KAONS*

Karol Lang †

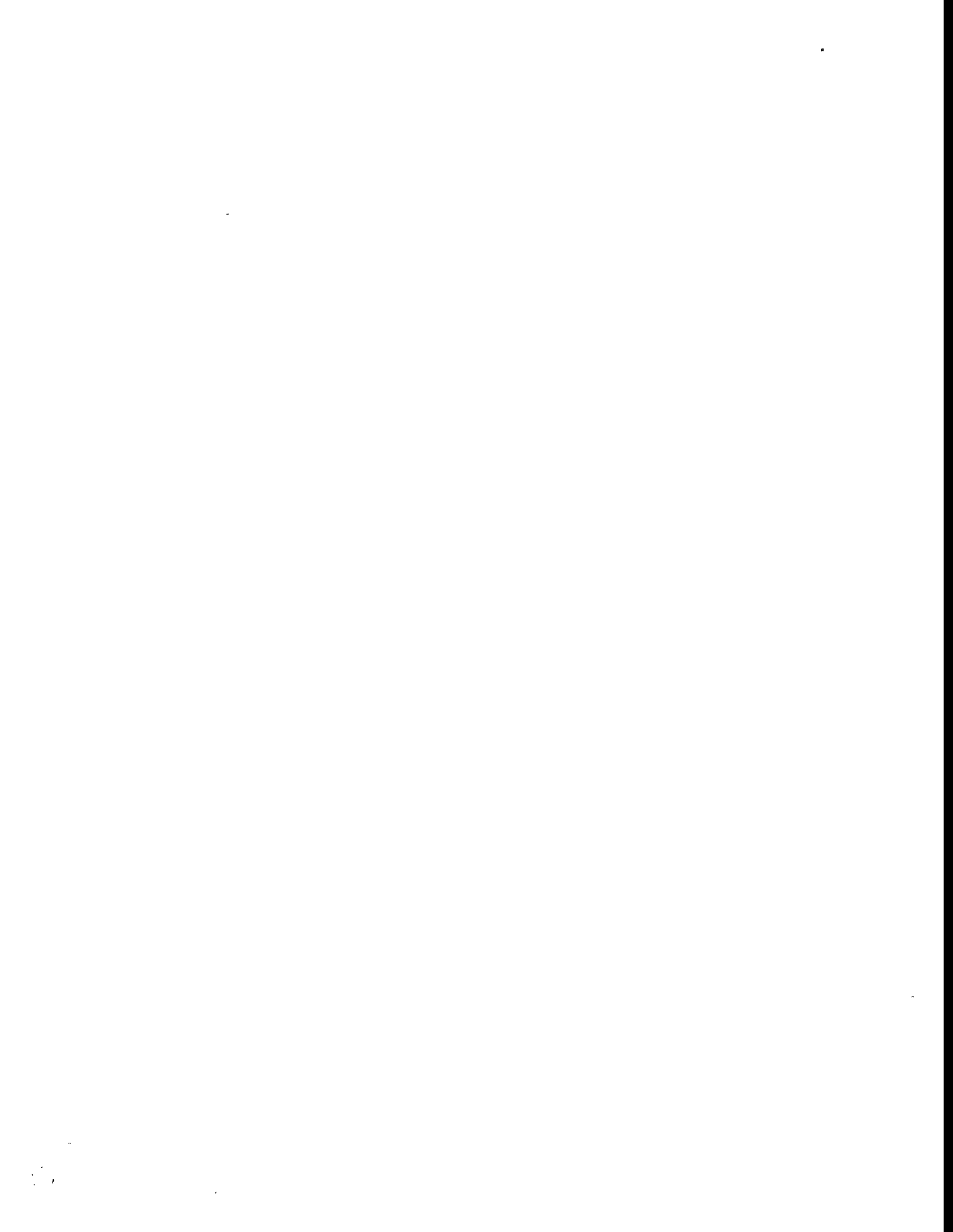
*Department of Physics
University of Texas at Austin
Austin, Texas 78712*

DISCLAIMER

This report was prepared as an account of work sponsored by an agency of the United States Government. Neither the United States Government nor any agency thereof, nor any of their employees, makes any warranty, express or implied, or assumes any legal liability or responsibility for the accuracy, completeness, or usefulness of any information, apparatus, product, or process disclosed, or represents that its use would not infringe privately owned rights. Reference herein to any specific commercial product, process, or service by trade name, trademark, manufacturer, or otherwise does not necessarily constitute or imply its endorsement, recommendation, or favoring by the United States Government or any agency thereof. The views and opinions of authors expressed herein do not necessarily state or reflect those of the United States Government or any agency thereof.

*Invited talk presented at The 1995 SLAC Summer Institute's Topical Conference, SLAC, July 20, 1995; to appear in the Proceedings.

†Supported by DOE Contract DE-FG03-93ER-40757 (Task OJI).



UTEXAS-HEP-95-18
DOE-ER40757-074

SEARCHES FOR VERY RARE DECAYS OF KAONS*

Karol Lang [†]

*Department of Physics
University of Texas at Austin
Austin, Texas 78712*

ABSTRACT

The physics motivation for searches for very rare kaon decays, either forbidden or suppressed within the Standard Model, is briefly discussed. Simple arguments conclude that such searches probe possible new forces at a 200 TeV mass scale or constitute a precision test of the electroweak model. The examples of such processes are decays of $K_L^0 \rightarrow \mu^\pm e^\mp$, $K^+ \rightarrow \pi^+ \mu^+ e^-$, $K_L^0 \rightarrow \mu^+ \mu^-$, and $K^+ \rightarrow \pi^+ \nu \bar{\nu}$. We present the current experimental status and describe the new efforts to reach sensitivities down to 1 part in 10^{12} . The discussion is focused on the experimental program at the Alternating Gradient Synchrotron at Brookhaven National Laboratory, where intense beams make such studies possible.

*Invited talk presented at The 1995 SLAC Summer Institute's Topical Conference, SLAC, July 20, 1995; to appear in the Proceedings.

[†]Supported by DOE Contract DE-FG03-93ER-40757 (Task OJI).

1 Introduction

Experimental confirmations of a theoretical picture of elementary interactions, the Standard Model, constitute an undeniable triumph of particle physics. Despite that, the Standard Model is generally perceived as incomplete or merely a *low* energy realization of a more general theory with a full symmetry at some high energy. There are indeed many basic questions regarding the Standard Model to which answers will have to come from the outside of the model. With 21 free parameters in the minimal version of the Model an overall picture is complicated and many *fundamental* questions are obvious: Why are there three quark and lepton families? Why is the number of families three in both cases? Why are the masses of constituent fermions and intermediate bosons what they are? Why and how is CP violated? Why is separate lepton-flavor conserved? etc...

As the consequence of this situation, many new theoretical models (or entire classes of models) have been proposed over the years. The most successful ones (i.e., the ones which have survived the challenge of existing experimental data and make (usually hard to test) predictions of new phenomena) include supersymmetry,¹ technicolor,² left-right symmetry,³ horizontal symmetry,⁴ compositeness,⁵ and the most hopeful candidate for the ultimate theory of elementary particles, superstring theory.⁶ At the same time testing of the Standard Model continues by examining more and more subtle effects predicted by it. One such venue is studying higher-order electroweak (i.e., suppressed) processes. The level at which they occur subjects the theory to a stringent scrutiny and may lead to observed inconsistencies pointing towards “new physics”. Processes like $K^+ \rightarrow \pi^+ \nu \bar{\nu}$, $K_L^0 \rightarrow \mu^+ \mu^-$, and $K_L^0 \rightarrow e^+ e^-$ could be used both ways: to confirm or to look beyond the Standard Model. They can shed light on the CP-violation mechanism – one of the crucial tests of the present theory.

Looking back at the history of elementary particles one cannot escape a conclusion that kaons played a central role in many discoveries. Starting with associated (strangeness) production and “ $\tau - \theta$ puzzle”, through CP-violation, and GIM-mechanism, the kaon system was essential in establishing the foundations of the Standard Model. Studies of rare kaon decays continue this physics-rich tradition. Rare processes provide sensitive tests of new theories and an important testing ground for the Standard Model. The field of rare decays is diverse and active as it offers potential for major discoveries. At the Alternating Gradient

Synchrotron (AGS) at Brookhaven National Laboratory (BNL) the program is centered around tests of the separate lepton-flavor conservation ($K_L^0 \rightarrow \mu^\pm e^\mp$, $K^+ \rightarrow \pi^+ \mu^+ e^-$, $\pi^0 \rightarrow \mu^\mp e^\pm$), and measurements of the suppressed electroweak decays ($K^+ \rightarrow \pi^+ \nu \bar{\nu}$, $K_L^0 \rightarrow \mu^+ \mu^-$). The newest generation of detectors optimized for these decays is completed, and now the AGS program is entering the extended data-taking period.

This review focuses on searches and studies of processes pursued by experiments at BNL. Transitions relevant for the CP-violation (like $K_L^0 \rightarrow \pi^0 e^+ e^-$) are primarily studied at other laboratories and will not be covered here. Some other recent articles offer more complete overviews^{7,8,9,10} .

2 Motivation

2.1 Forbidden Processes

Many new theories, or “extensions” of the Standard Model, predict observation of separate lepton-flavor violation. In variety of theories, as illustrated in Figure 1, processes like $K_L^0 \rightarrow \mu^\pm e^\mp$ or $K^+ \rightarrow \pi^+ \mu^+ e^-$ occur at tree-level. Such decays are forbidden within the Standard Model although the origin of separate lepton-flavor conservation is not understood. It is not associated with any known symmetry usually expected to exist behind a conservation law. Decays $K_L^0 \rightarrow \mu^\pm e^\mp$ or $K^+ \rightarrow \pi^+ \mu^+ e^-$ have to be mediated by a *new* intermediate boson thus explicitly manifesting *a new fundamental force* in Nature. As such, these processes comprise some of the most sensitive tests of new theories.

Figure 1 illustrates how some models lead naturally to $K_L^0 \rightarrow \mu^\pm e^\mp$. To construct “a dimensional argument” one can assume a $V - A$ form of a new interaction and compare it to a copious electroweak decay $K^+ \rightarrow \mu^+ \nu_\mu$ as shown in Figure 2:

$$\frac{\Gamma(K_L^0 \rightarrow \mu^\pm e^\mp)}{\Gamma(K^+ \rightarrow \mu^+ \nu_\nu)} \simeq \left[\frac{ff'/M_X^2}{g^2 \sin \theta_C / M_W^2} \right]^2 \quad (1)$$

where θ_C is the Cabibbo angle, M_W the mass of the W boson, and g is the electroweak coupling. Thus the branching ratio is

$$B(K_L^0 \rightarrow \mu^\pm e^\mp) = \frac{\Gamma(K_L^0 \rightarrow \mu^\pm e^\mp)}{\Gamma(K_L^0 \rightarrow \text{all})} \simeq \frac{\Gamma(K^+ \rightarrow \mu^+ \nu_\mu)}{\Gamma(K_L^0 \rightarrow \text{all})} \left[\frac{ff'/M_X^2}{g^2 \sin \theta_C / M_W^2} \right]^2 \quad (2)$$

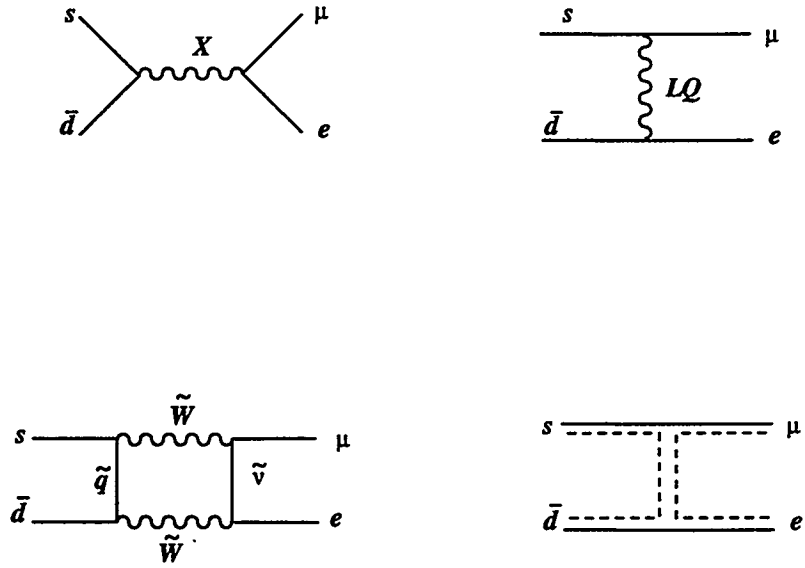


Figure 1: Examples of tree-level diagrams leading to the separate lepton-flavor violation in four classes of theories “beyond” the Standard Model: (a) horizontal symmetry, (b) leptoquarks, (c) supersymmetry, (d) compositeness.

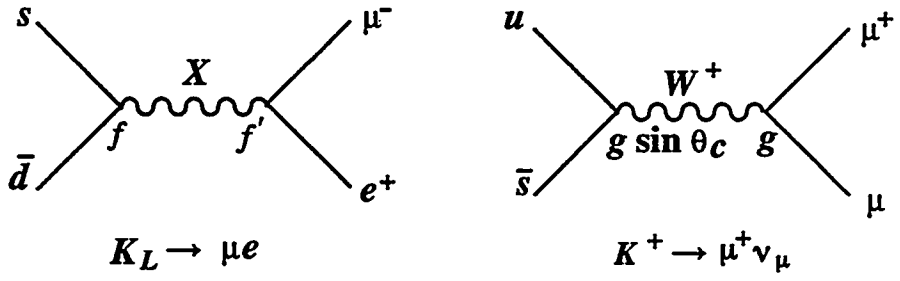


Figure 2: Examples of a tree-level diagram with “horizontal symmetry” leading to the separate lepton-flavor violation $K_L^0 \rightarrow \mu^\pm e^\mp$, and a copious electroweak decay $K^+ \rightarrow \mu^+ \nu_\mu$.

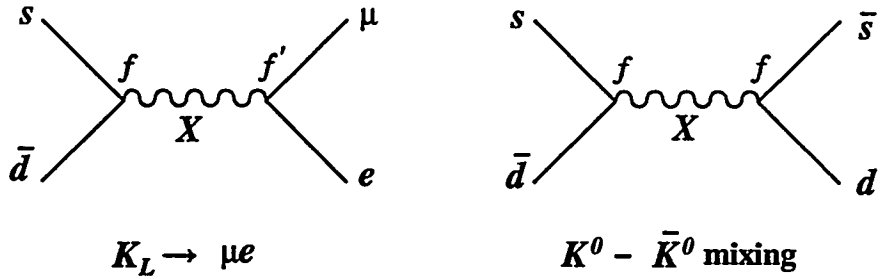


Figure 3: A diagram with “horizontal symmetry” leading to the separate lepton-flavor violation $K_L^0 \rightarrow \mu^\pm e^\mp$ could also contribute to $K^0 \leftrightarrow \bar{K}^0$.

Inserting the known numbers gives

$$B(K_L^0 \rightarrow \mu e) \simeq (1.2 \times 10^{-2} \text{TeV}^4) \left[\frac{f^2}{M_X^2} \right]^2 \left[\frac{f'}{f} \right]^2 . \quad (3)$$

Assuming for simplicity the same couplings $f = f' = g$ turns this comparison to a specific relationship of branching fractions versus the mass scale of the new interaction

$$M_X \simeq 220 \text{TeV} \left[\frac{10^{-12}}{B(K_L^0 \rightarrow \mu e)} \right]^{1/4} . \quad (4)$$

A similar comparison between $K^+ \rightarrow \pi^+ \mu^+ e^-$ and $K_L^0 \rightarrow \pi^\pm \mu^\mp \nu_\mu$ yields

$$M_X \simeq 86 \text{TeV} \left[\frac{10^{-12}}{B(K^+ \rightarrow \pi^+ \mu^\pm e^\mp)} \right]^{1/4} . \quad (5)$$

Thus sensitivity to *rare* processes opens a window at interactions at *very high mass scales* through virtual effects of *new particles*. It should be emphasized that $K_L^0 \rightarrow \mu^\pm e^\mp$ and $K^+ \rightarrow \pi^+ \mu^+ e^-$ provide complementary information on potential new interactions. The first is sensitive to axial-vector or pseudoscalar couplings, the second is sensitive to vector or scalar couplings.

For completeness it is worth mentioning that a new force in $K_L^0 \rightarrow \mu^\pm e^\mp$ may also contribute to $K^0 \leftrightarrow \bar{K}^0$ transitions as illustrated in Figure 3. Thus stringent limits on M_X from Δm_K exist. However, some theories circumvent this restriction.¹¹ If one assigns “a generation number”, G , to leptons and quarks with $G = 1$ for (e, ν_e, u, d) , $G = 2$ for (μ, ν_μ, c, s) , and $G = 3$ for (τ, ν_τ, t, b) , then $K_L^0 \rightarrow \mu^\pm e^\mp$ is a $\Delta G = 0$, and $K^0 \leftrightarrow \bar{K}^0$ is $|\Delta G| = 2$ transition. If G is conserved by the new force (representing some unknown symmetry) $K_L^0 \rightarrow \mu^\pm e^\mp$ would be allowed without affecting $K^0 \leftrightarrow \bar{K}^0$.

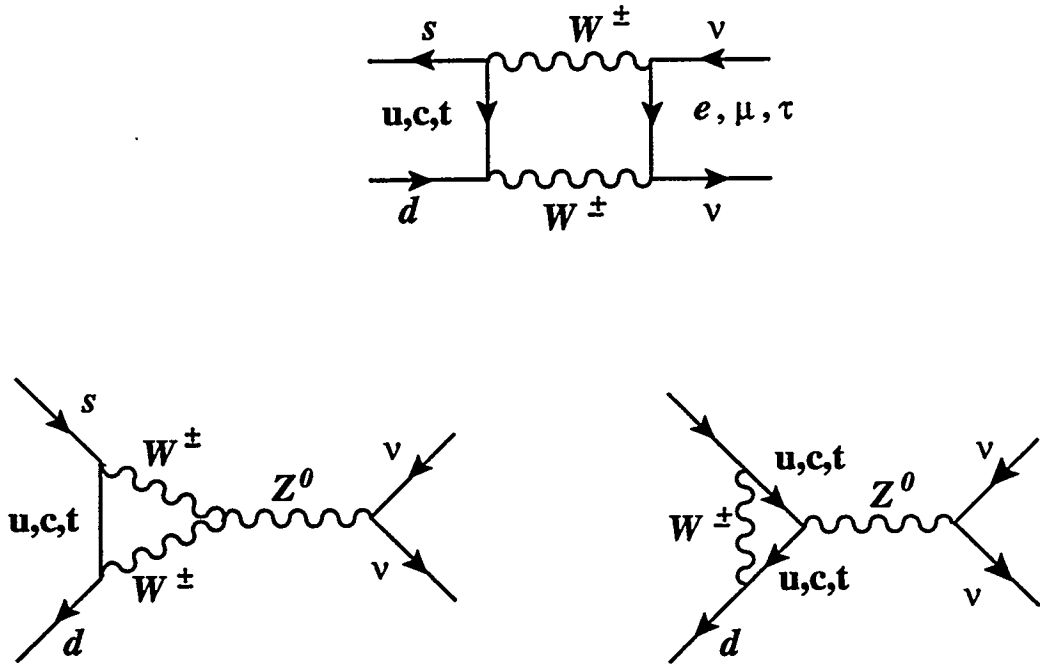


Figure 4: Short-distance diagrams which dominate the transition $K^+ \rightarrow \pi^+ \nu \bar{\nu}$.

2.2 Suppressed Processes

Decays proceeding through a higher-order (loop-level) electroweak transition constitute an essential test of the Standard Model. Rates of decays such as $K^+ \rightarrow \pi^+ \nu \bar{\nu}$ or $K_L^0 \rightarrow \mu^+ \mu^-$ (referred to as Flavor-Changing Neutral Currents (FCNC)) could be used as a check of the theory, or to extract some of the parameters of the theory which are hard to reach through other processes.

The $K^+ \rightarrow \pi^+ \nu \bar{\nu}$ decay mode is short-distance *dominated*^{12,13,14,15} and proceeds mainly via diagrams shown in Figure 4. With QCD corrections known and small,¹⁶ the diagrams depend primarily on the mass of the charm and top quarks, m_t and m_c , and the $V_{ts}^* V_{td}$ product of the elements of the Cabibbo-Kobayashi-Maskawa (*CKM*) mixing matrix. If all uncertainties are included the $B(K^+ \rightarrow \pi^+ \nu \bar{\nu})$ is expected in the range of $(0.5-5.0) \times 10^{-10}$. Thus, if observed, the process can be used to shed more light on m_t and the *CKM* matrix.

$K_L^0 \rightarrow \mu^+ \mu^-$ mode has played a crucial role in establishing the multi-family quark content of the theory through the famous Glashow-Iliopoulos-Maiani cancellation (“GIM-mechanism”).¹⁷ The reaction is dominated by an electromagnetic two-(on-shell)photon transition, as shown in Figure 5a, which determines the uni-

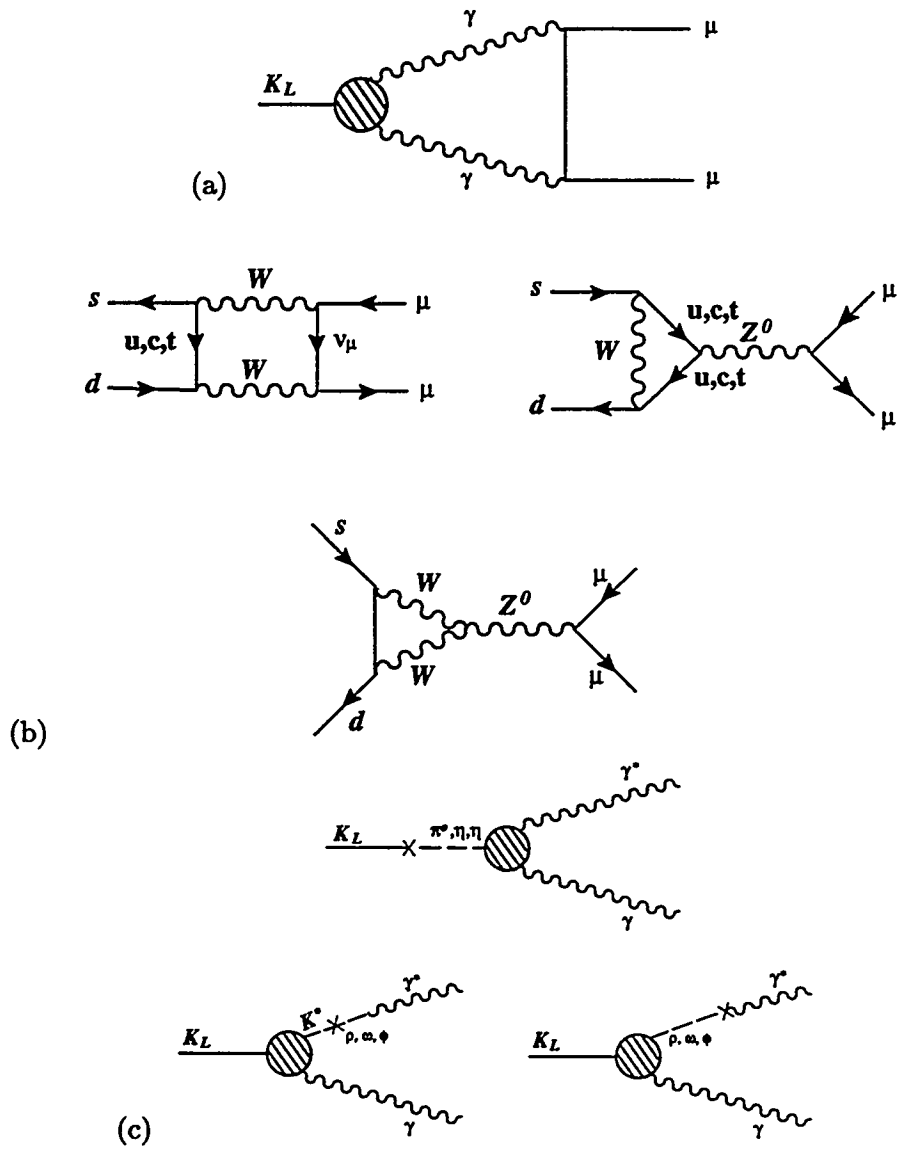


Figure 5: Diagrams contributing to $K_L^0 \rightarrow \mu^+ \mu^-$: a) a dominant diagram which determines the unitarity boundary for this process at $(6.8 \pm 0.3) \times 10^{-9}$, b) short-distance “box” and “penguin” diagrams (similar to $K^+ \rightarrow \pi^+ \nu \bar{\nu}$), and c) representation of long-distance contributions.

tarity bound for the branching fraction¹⁸

$$\frac{\Gamma(K_L^0 \rightarrow \mu\mu)_{2\gamma}}{\Gamma(K_L^0 \rightarrow \gamma\gamma)} = \alpha^2 \left(\frac{m_\mu}{m_K} \right)^2 \frac{1}{2\beta} \left(\ln \frac{1+\beta}{1-\beta} \right)^2 , \quad (6)$$

where $\beta = \sqrt{1 - 4m_\mu^2/m_K^2}$. The numerical uncertainty of this process is primarily due to the experimental uncertainty of $B(K_L^0 \rightarrow \gamma\gamma)$, measured to be¹⁹ $B(K_L^0 \rightarrow \gamma\gamma) = (5.70 \pm 0.27) \times 10^{-4}$. So

$$B(K_L^0 \rightarrow \mu\mu)_{2\gamma} = (1.2 \times 10^{-5}) B(K_L^0 \rightarrow \gamma\gamma) = (6.8 \pm 0.3) \times 10^{-9} . \quad (7)$$

There are also other contributions to this transition: the short-distance diagrams^{20,21} shown in Figure 5b (similar to the $K^+ \rightarrow \pi^+ \nu\bar{\nu}$ diagrams in Figure 4 where neutrino lines are replaced with muon lines), and the long-distance diagrams exemplified by graphs in Figure 5c.

At present, it is not clear how to calculate the long-distance contributions with uncertainties small enough to extract the short-distance graphs^{22,23} and thus obtain information on m_t and V_{td} . However, theoretical and experimental efforts are under way to improve this situation. Determination of $K_L^0 - \gamma^* - \gamma$ and $K_L^0 - \gamma^* - \gamma^*$ vertices from such decays as $K_L^0 \rightarrow e^+ e^- \gamma$, $K_L^0 \rightarrow \mu^+ \mu^- \gamma$, and $K_L^0 \rightarrow e^+ e^- e^+ e^-$ should provide additional guidance for the chiral perturbation theory so that the extraction of the short-distance part of $K_L^0 \rightarrow \mu^+ \mu^-$ may be feasible.

In summary, the two decay modes $K^+ \rightarrow \pi^+ \nu\bar{\nu}$ and $K_L^0 \rightarrow \mu^+ \mu^-$ are complementary: $K^+ \rightarrow \pi^+ \nu\bar{\nu}$ is harder experimentally, but cleaner theoretically; $K_L^0 \rightarrow \mu^+ \mu^-$ is presently less well understood theoretically, but the near future should bring thousands of collected events.

2.3 Searches for New Particles and Other Rare Decays

As a byproduct of searches for rare decays of kaons, other channels are studied. In particular modes like $K^+ \rightarrow \pi^+ X^0$, where X^0 is a new particle could be examined. Particular experimental approaches impose certain sensitivity windows for masses and lifetimes of such new objects. In addition, hermeticity and acceptances of spectrometers allow also searches for other rare decays like $\pi^0 \rightarrow \mu^\mp e^\pm$ or measurement of $\pi^0 \rightarrow e^+ e^-$.

Other less rare decay channels like $K^+ \rightarrow \pi^+ e^+ e^-$, $K^+ \rightarrow \pi^+ \mu^+ \mu^-$, $K^+ \rightarrow \pi^+ \gamma\gamma$, $K^+ \rightarrow \pi^+ \pi^0 e^+ e^-$, $K^+ \rightarrow e^+ e^+ e^- \nu$, $K^+ \rightarrow \mu^+ e^+ e^- \nu$,

$K^+ \rightarrow \pi^+ \pi^0 \gamma$, $K^+ \rightarrow \mu^+ \nu_\mu \gamma$, and $K^+ \rightarrow \pi^0 \mu^+ \nu_\mu \gamma$ are also pursued, and could either present more stringent tests of the chiral perturbation theory or provide additional input to advance it for processes like $K_L^0 \rightarrow \mu^+ \mu^-$.

3 Current Best Results

Searches for rare kaon decays have had a very long tradition. As illustrated in Figures 6 and 7 the progression of new results is grouped in two time periods. In late 1960's to early 1970's, experiments impressively probed branching ratios down to 10^{-8} level. Exhausting detector technology and available beam intensities the searches stagnated for about a decade. They were renewed in the early 1980's when more modern experiments were able to provide faster and better detectors and data acquisition, and more intense beams became available. Most of final results from these recent searches have been published. Tables 1, 2, and 3 list these results. Figures 8, 9, 10, and 11 illustrate some of the results in a full form as published.

The lowest sensitivities have been reached at the AGS at BNL. Results from KEK played an important role in the early stages of the new generation experiments, but have been ultimately superseded by the BNL experiments. As this round of experiments exploited the detector and beam capabilities, the three groups at BNL, equipped with multi-year experience of conducting experiments with intense beams, embarked on the next round of studies.

The newest upgrades and follow-up experiments have been designed with goals to reach sensitivities which would "close the discovery window" for allowed pro-

Decay mode	90% C.L. limit	Reference
$K_L^0 \rightarrow \mu^\pm e^\mp$	$< 3.3 \times 10^{-11}$	BNL E791 ²⁴
	$< 9.4 \times 10^{-11}$	KEK E137 ²⁵
	$< 1.9 \times 10^{-9}$	BNL E780 ²⁶
$K^+ \rightarrow \pi^+ \mu^+ e^-$	$< 2.1 \times 10^{-10}$	BNL 777 ²⁷
$K^+ \rightarrow \pi^+ X^0$	$< 5.2 \times 10^{-10}$ X^0 weakly interacting	BNL 787 ²⁸

Table 1: Summary of best limits of searches beyond the Standard Model.

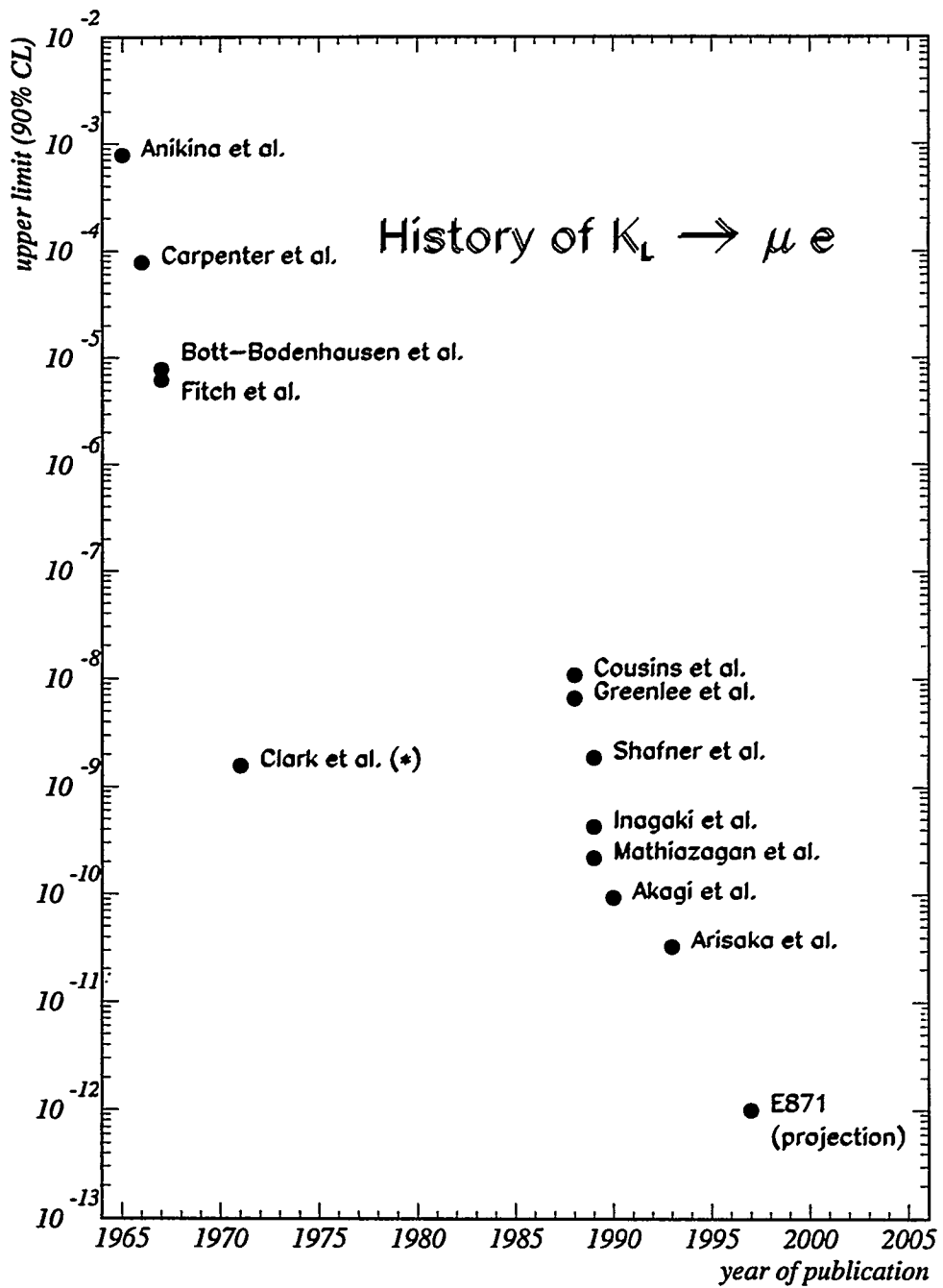


Figure 6: History of $K_L^0 \rightarrow \mu^\pm e^\mp$ searches¹⁹. The result of Clark *et al.* has possible (but unknown) systematic error. The points represent 90% C.L. upper limits.

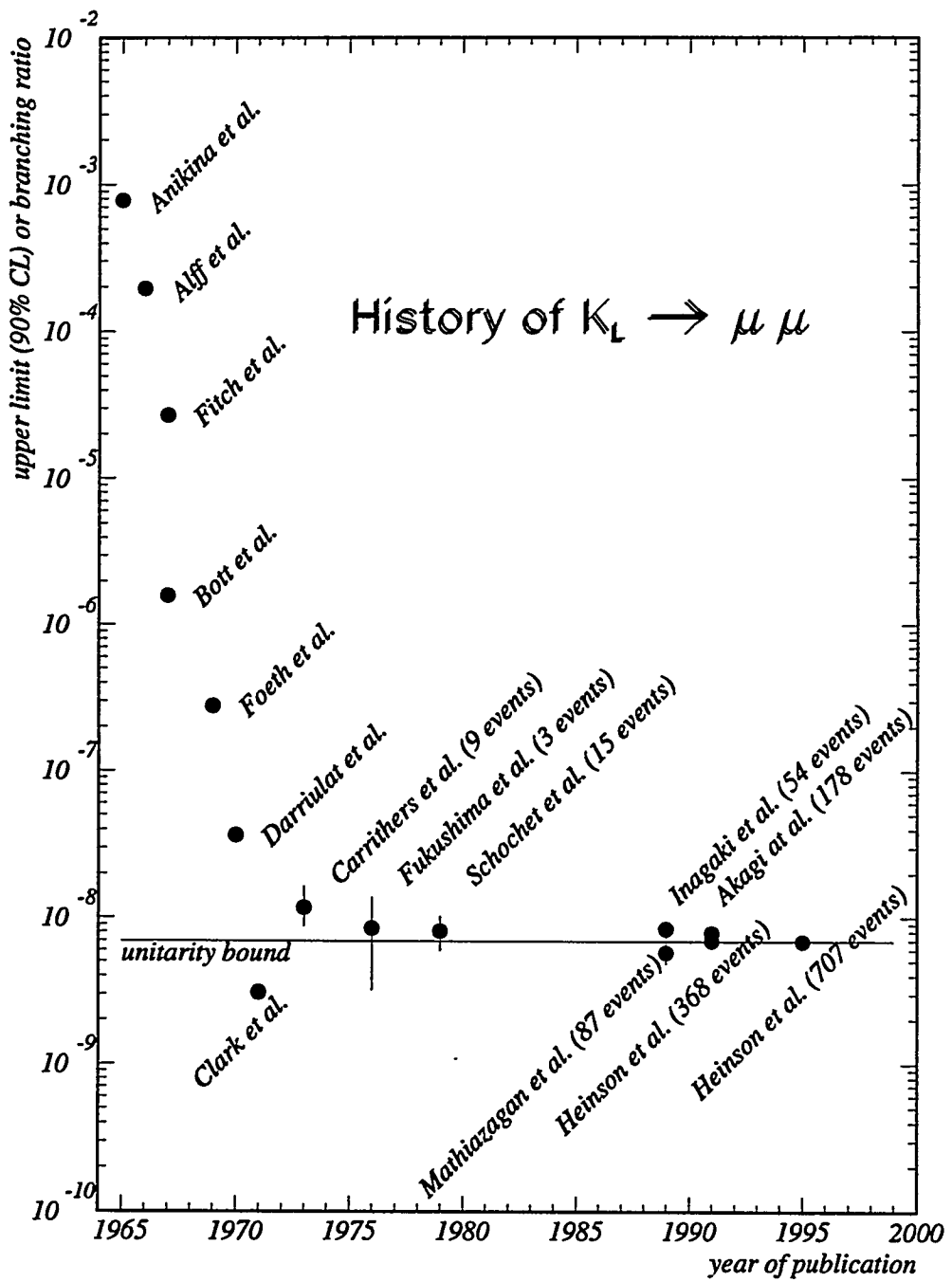


Figure 7: History of $K_L^0 \rightarrow \mu^+ \mu^-$ results¹⁹. The first observation of this decay was reported by Carrithers *et al.* in 1973, thus the earlier points represent 90% C.L. upper limits.

Decay mode	BR or 90% C.L. limit	Reference
$K^+ \rightarrow \pi^+ \nu \bar{\nu}$	$< 2.4 \times 10^{-9}$	BNL E787 ²⁸
$K_L^0 \rightarrow \mu^+ \mu^-$	$(6.86 \pm 0.37) \times 10^{-9}$	BNL E791 ²⁹
	$(7.9 \pm 0.6(stat.) \pm 0.3(sys.)) \times 10^{-9}$	KEK E137 ³⁰
$K_L^0 \rightarrow e^+ e^-$	$< 4.1 \times 10^{-11}$	BNL E791 ³¹
	$< 1.6 \times 10^{-10}$	KEK E137 ²⁵
	$< 1.2 \times 10^{-9}$	BNL E780 ³²

Table 2: Summary of best results on processes suppressed within the Standard Model.

Decay mode	BR or 90% C.L. limit	Reference
$K^+ \rightarrow \pi^+ X^0$	$< 1.5 \times 10^{-8*}$	BNL E851 ³³
$X^0 \rightarrow e^+ e^-$	$150 \text{ MeV} < m_{X^0} < 340 \text{ MeV}$	
$K^+ \rightarrow \pi^+ X^0$	$< 1.6 \times 10^{-6}$	BNL E787 ³⁴
$X^0 \rightarrow \gamma \gamma$	$0 \text{ MeV} < m_{X^0} < 150 \text{ MeV}$	
$K^+ \rightarrow \pi^+ \gamma \gamma$	$< 1.0 \times 10^{-6}$	BNL E787 ³⁴
$K^+ \rightarrow \pi^+ H^0$	$< 1.5 \times 10^{-7}$	BNL E787 ³⁵
$H \rightarrow \mu^+ \mu^-$	$220 \text{ MeV} < m_{X^0} < 320 \text{ MeV}$	
$\pi^0 \rightarrow \mu^\mp e^\pm$	$< 1.6 \times 10^{-8}$	BNL E777 ²⁷
$K^+ \rightarrow \pi^+ e^+ e^-$	$(2.75 \pm 0.23(stat.) \pm 0.13(sys.)) \times 10^{-7}$	BNL E851 ³³
$\pi^0 \rightarrow e^+ e^-$	$(6.9 \pm 2.3(stat.) \pm 0.6(sys.)) \times 10^{-8}$	BNL E851 ³⁶
$\pi^0 \rightarrow e^+ e^-$ $(m_{ee}/m_{\pi^0})^2 > 0.95$	$(7.6^{+3.9}_{-2.8}(stat.) \pm 0.5(sys.)) \times 10^{-8}$	FNAL E799 ³⁷

Table 3: Summary of other searches and limits from the rare K decay experiments. (* 99% C.L.)

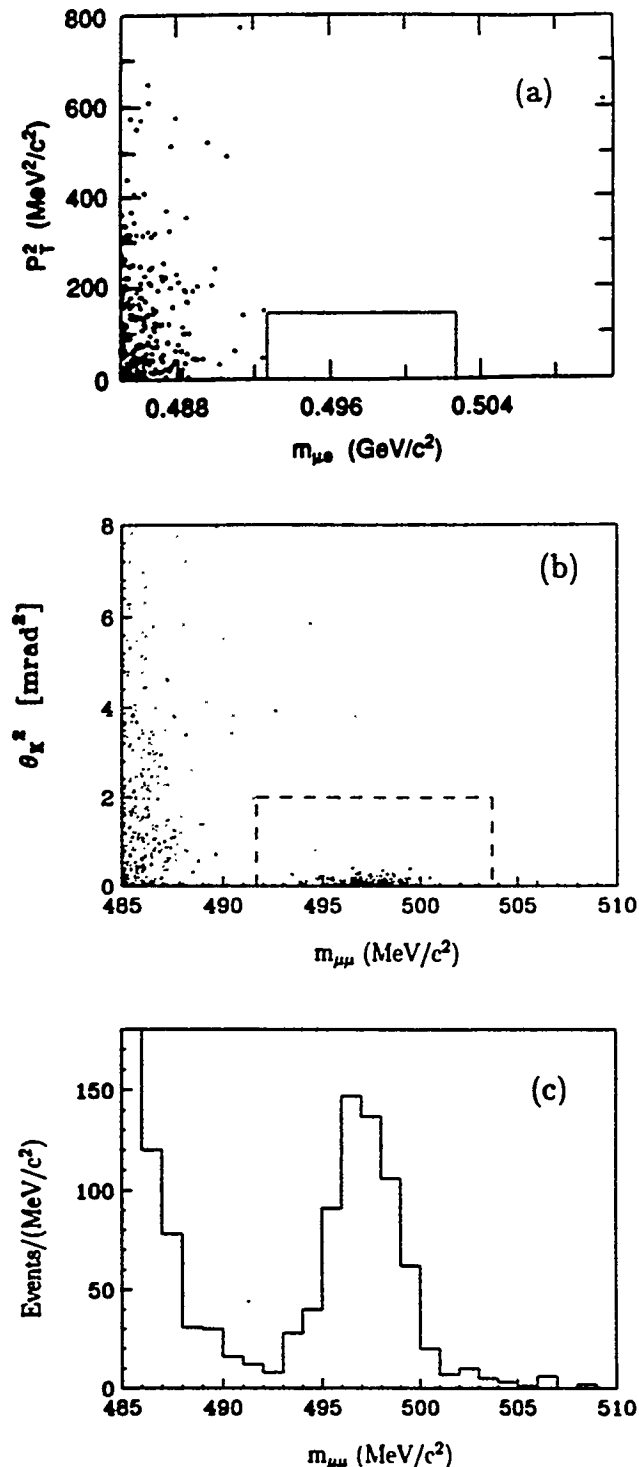


Figure 8: Final results from BNL E791. The top figure is a scatter plot of p_T^2 versus $M_{\mu e}$ for $K_L^0 \rightarrow \mu^\pm e^\mp$ candidates²⁴ (p_T is a missing transverse momentum of the reconstructed final-state pair). The bottom figure shows the $K_L^0 \rightarrow \mu^+ \mu^-$ mass peak of > 700 events²⁹ (an angle θ_K points in the direction of the missing transverse momentum, and is equivalent to p_T). The rectangular signal boxes surround $M_K = 0.497$ MeV/c 2 and $p_T = 0$ (or $\theta_K = 0$).

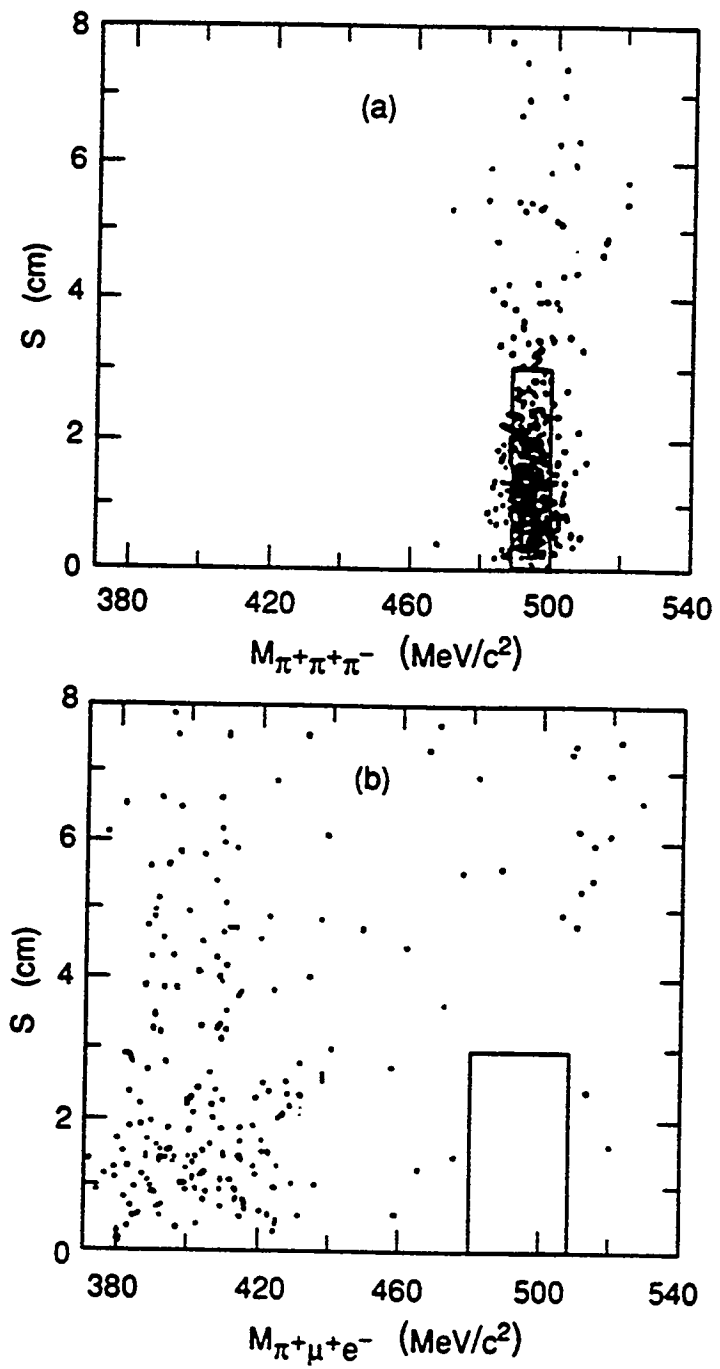


Figure 9: Final results from BNL E777. The scatter plots of the variable S vs invariant mass (S is the rms distance of closest approach of three track combinations to a common vertex). The top figure shows $K^+ \rightarrow \pi^+\pi^-\pi^0$ decays; the bottom $K^+ \rightarrow \pi^+\mu^+e^-$ candidates²⁷.

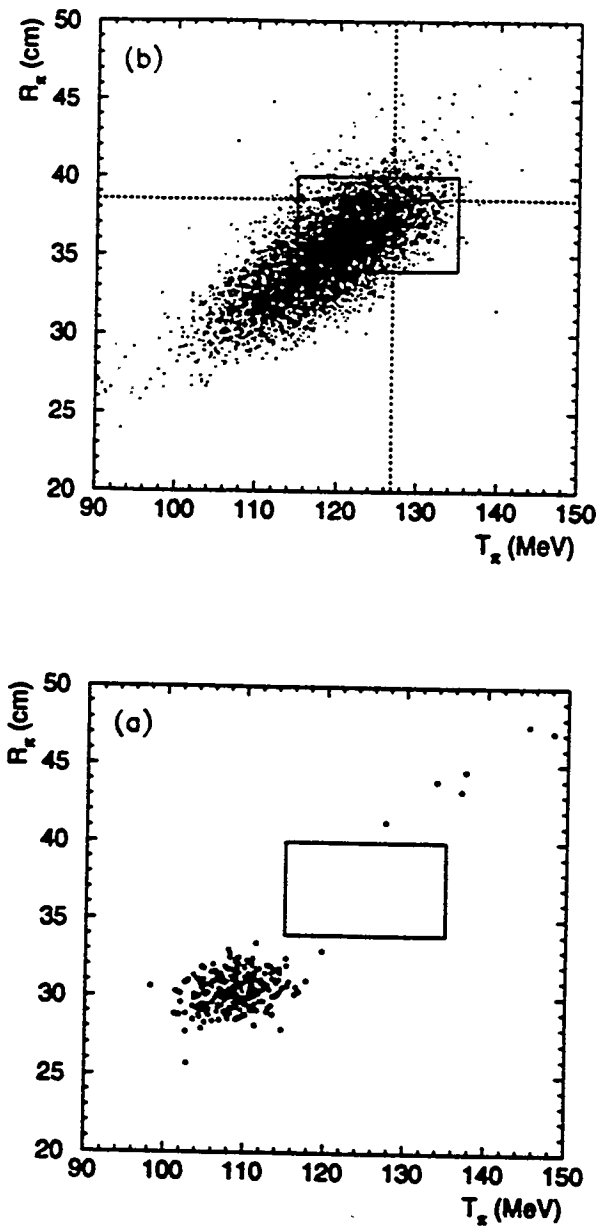


Figure 10: Final results from BNL E787. Charged-track range versus kinetic energy for (a) data and (b) $K^+ \rightarrow \pi^+ \nu \bar{\nu}$ Monte Carlo for events satisfying the selection criteria and having measured momentum $211 \leq P_\pi \leq 243$ MeV/c. The rectangular box indicates the search region for $K^+ \rightarrow \pi^+ \nu \bar{\nu}$ and $K^+ \rightarrow \pi^+ X^0$ ($M_{X^0} \approx 0$). The horizontal and vertical dashed lines in (b) are the theoretical end-points of $K^+ \rightarrow \pi^+ \nu \bar{\nu}$ in range and energy, respectively²⁸.

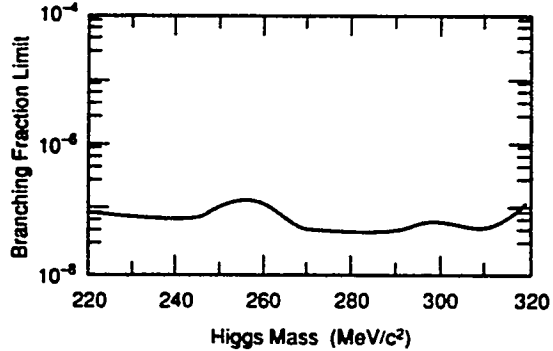
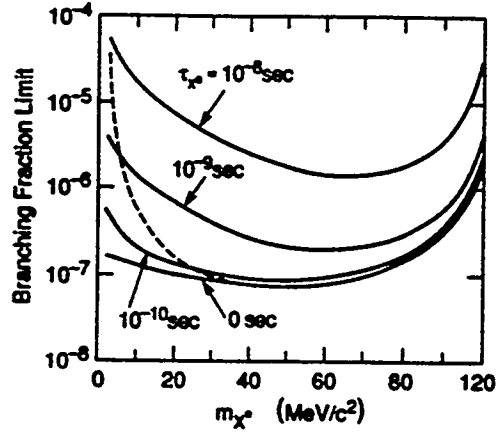
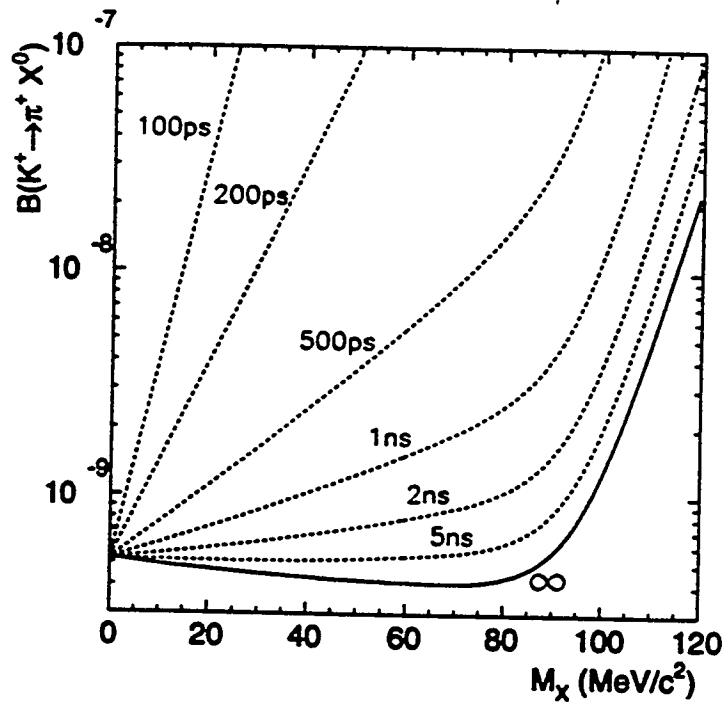


Figure 11: Limits from the other searches from BNL E787: (a) the 90% C.L. upper limits on $B(K^+ \rightarrow \pi^+ X^0)$ as a function of M_{X^0} and various X^0 lifetimes²⁸; (b) the 90% C.L. upper limit on $K^+ \rightarrow \pi^+ H^0$ with $H \rightarrow \mu\mu$ as a function of m_H ³⁵; (c) the 90% C.L. upper limit on $K^+ \rightarrow \pi^+ X^0$ with $X^0 \rightarrow \gamma\gamma$ for different X^0 lifetimes as a function of mass m_{X^0} . The dashed curve shows the upper limit for the combined branching ratio $K^+ \rightarrow \pi^+ H^0$ and $H^0 \rightarrow \gamma\gamma$ ³⁴.

cesses ($K^+ \rightarrow \pi^+ \nu \bar{\nu}$ and $K_L^0 \rightarrow e^+ e^-$), and probe branching fractions at the 10^{-12} level ($K_L^0 \rightarrow \mu^\pm e^\mp$ and $K^+ \rightarrow \pi^+ \mu^+ e^-$). The new experiments have been commissioned and started data-taking period which will extend into the near future. In the following part of this article these experimental efforts will be briefly discussed.

4 Experiments in Progress

4.1 AGS

Alternating Gradient Synchrotron at BNL provides the beam for the rare kaon experiments. The accelerator was commissioned in 1960 and originally provided 10^{10} protons per pulse. The AGS has been continuously upgraded, conforming to new technology and new experimental requirements. The ~ 250 m diameter synchrotron ring can now accelerate protons (up to 33 GeV/c, but more reliably at 24 GeV/c), polarized protons (up to 22 GeV/c) and heavy ions (gold ions up to 14.5 GeV/c per nucleon). In the future, the AGS complex will provide an injector system to the Relativistic Heavy Ion Collider (RHIC) currently under construction.

The AGS has recently completed another phase of upgrades - construction of a new rf system and an injector ring, known as the Booster. The Booster increases the proton energy for injection to the AGS from 0.2 GeV to 1.5 GeV, and quadruples the AGS intensity by using four bunches in one AGS acceleration cycle. The new intensity record of 6.3×10^{13} protons per pulse was reached during the 1995 proton run and exceeds the design goal. The 24 GeV/c primary proton beam is delivered about every 3.2-3.6 seconds over 1.2-1.6 second long "slow" extraction, assuring about 40% duty cycle. Essentially the entire *new* AGS intensity is necessary to support adequately the kaon program.

4.2 The $K_L^0 \rightarrow \mu^\pm e^\mp$ experiment (E871)

The primary goal of E871^{38,39} is to search for separate lepton-flavor violation in the decay $K_L^0 \rightarrow \mu^\pm e^\mp$. The two-arm spectrometer is optimized for this search and should reach a single event sensitivity of 10^{-12} , probing new forces in nature in the 200 TeV mass range. Other decays, such as $K_L^0 \rightarrow \mu^+ \mu^-$, and

$K_L^0 \rightarrow e^+e^-$ can also be studied. For the former, a sample of several thousand decays is expected to be recorded. For the latter, predicted by the Standard Model to occur at $\sim 3 \times 10^{-12}$ level, the experiment should detect the first few events ever.

The main source of background for $K_L^0 \rightarrow \mu^\pm e^\mp$ is the copious K_{e3} ($K_L^0 \rightarrow \pi^\pm e^\mp \nu_e$) decay which has a branching ratio $B(K_L^0 \rightarrow \pi^\pm e^\mp \nu_e) = 38.7\%$.¹⁹ If this decay proceeds in a way that the neutrino has very little energy in the laboratory frame, and the pion either decays $\pi \rightarrow \mu \nu_\mu$ or is misidentified as a muon, the *observed* final state contains a muon-electron pair. Theoretically, if experimental resolutions are ignored, the reconstructed invariant mass of the muon-electron pair, $M_{\mu e}$ could approach the mass of the parent kaon to within 8.4 MeV/c². Equally dangerous is the case when in $K_L^0 \rightarrow \pi^\pm e^\mp \nu_e$ decay *both* charged particles are misidentified. If the pion is mistaken by an electron, and the electron is mistaken for a pion, the invariant mass of this doubly-misidentified pair is not bounded by the kaon mass, M_K , and could exceed M_K if momentum of a pion is much larger than momentum of an electron. Analogously, the background for $K_L^0 \rightarrow \mu^+ \mu^-$ originates in (a) $K_L^0 \rightarrow \pi^\pm e^\mp \nu_e$ if $\pi \rightarrow \mu \nu_\mu$ and the electron is mistaken for a muon or (b) in $K_{\mu 3}$ decays $K_L^0 \rightarrow \pi^\pm \mu^\mp \nu_\mu$ ($B(K_L^0 \rightarrow \pi^\pm \mu^\mp \nu_\mu) = 27.0\%$ ¹⁹) if the pion decays or is mistaken for a muon. The background for $K_L^0 \rightarrow e^+e^-$ is due to $K_L^0 \rightarrow \pi^\pm e^\mp \nu_e$ with one of the pions mistaken for an electron, and, ironically, from other rare processes: $K_L^0 \rightarrow e^+e^-e^+e^-$ and $K_L^0 \rightarrow e^+e^-\gamma$ which occur at¹⁹ $(9.1 \pm 0.5) \times 10^{-6}$ and $(3.9 \pm 0.7) \times 10^{-8}$, respectively.

To reach 10^{-12} an experiment has to assure efficient background rejection. The essential requirements on an apparatus are good kinematics reconstruction and reliable particle identification, both to be accomplished in a high rate environment. The spectrometer for E871, shown in Figure 12, has been designed to satisfy such demands.³⁸ E871 is the successor to E791, which set a 90% C.L. upper limit for $B(K_L^0 \rightarrow \mu^\pm e^\mp)$ at 3.3×10^{-11} (see Table 1). The experiment has been fully commissioned for the 1995 AGS running cycle. The main features of the new apparatus, shown in Figure 12, are:

- two magnets for momentum-finding and providing “parallelism” (see below) of two-body decays
- a beam-stop placed in the first magnet to absorb the entire neutral beam

- redundant finely-segmented fast straw drift chambers and conventional drift chambers in regions of low rate
- redundant particle identification of muons and electrons
- multi-level trigger with fast on-line reconstruction
- fast custom-designed massively-parallel data acquisition system.

The neutral kaon beam is produced by an intense primary ~ 24 GeV/c beam of about 1.7×10^{13} protons delivered onto a (1.5-interaction-length) platinum target. A system of sweeping magnets and collimators placed at 3.75° with respect to the proton beam direction forms the neutral beam with mostly neutrons and kaons. Particles emerging from the 11 m long evacuated “decay volume” are tracked and identified in a two-magnet spectrometer. The neutral beam is absorbed in the beam stop specially designed and tested for this configuration.⁴⁰ The strengths of the magnetic fields (+440 MeV/c and -230 MeV/c) imposes that trajectories of two-body kaon decays emerge nearly parallel downstream of the second magnet. Such an arrangement simplifies triggering and provides the first rejection stage of the three-body decays. The intense primary proton beam produces $\sim 2 \times 10^7 K_L$ decays per the AGS pulse³⁸ resulting in high hit-rates in the upstream straw drift chambers. In addition, rates in chambers result from leakage of low energy particles (charged, neutrons and photons) from the beam-stop. The beam-stop shields the downstream part of the spectrometer, where the rates are substantially reduced. This minimizes the probability of pattern-recognition or particle-identification errors.

Particle identification of electrons and muons uses redundancy to minimize errors. Particles to be identified as electrons are required to have hits in a threshold Cerenkov counter filled with hydrogen (muons with momenta larger than 6.3 GeV/c and pions with momenta above 8.3 GeV/c can also produce Cerenkov radiation). In addition, electron candidates are identified with a segmented two-layer lead-glass calorimeter. Total energy deposited in lead-glass has to be consistent with the momentum measured from the reconstructed trajectory in the magnetic field. The $K_L^0 \rightarrow \pi^\pm e^\mp \nu_e$ and $K_L^0 \rightarrow \pi^\pm \mu^\mp \nu_\mu$ modes provide a constant calibration source for this system. Muons are identified as particles penetrating (the iron slabs in the upstream part and marble slabs in the remaining part of) the “muon range finder”. Scintillation hodoscopes are located at depths of material corresponding to muon momenta of 0.75, 0.94, 1.4, 2.8, and 5.8 GeV/c.

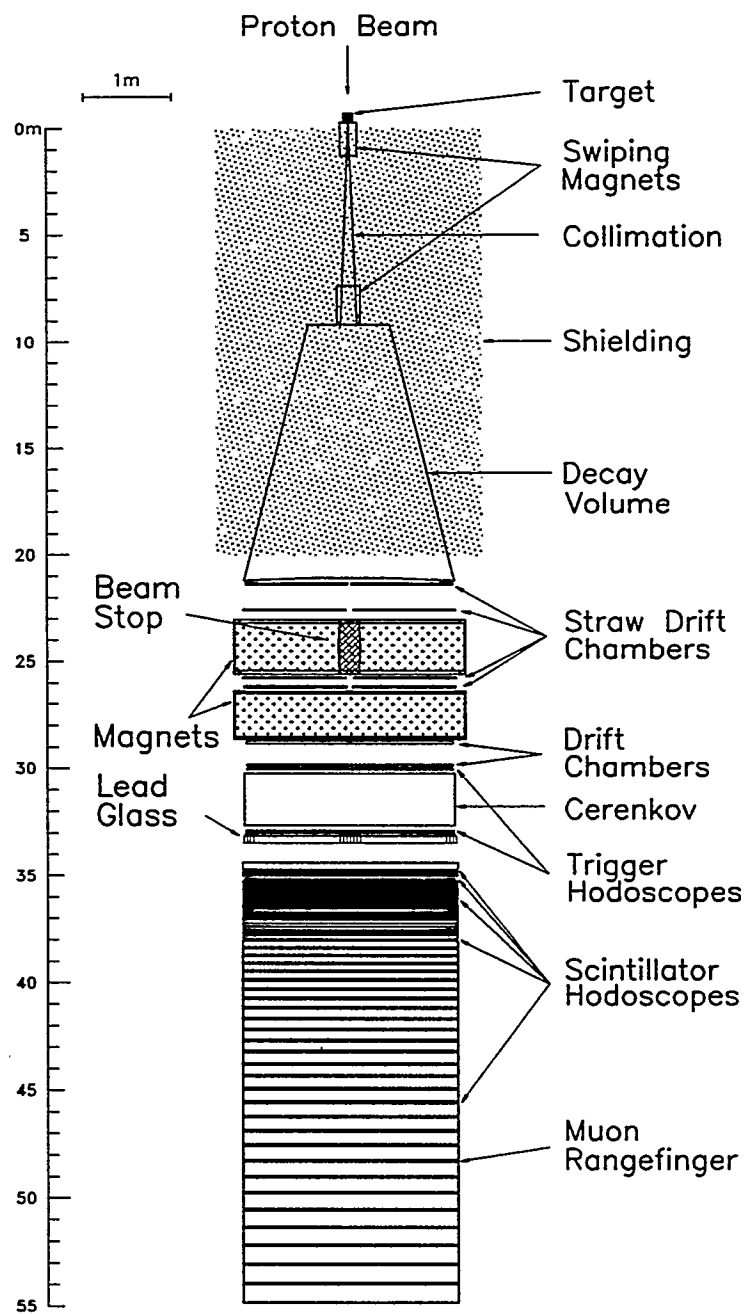


Figure 12: BNL E871 apparatus.

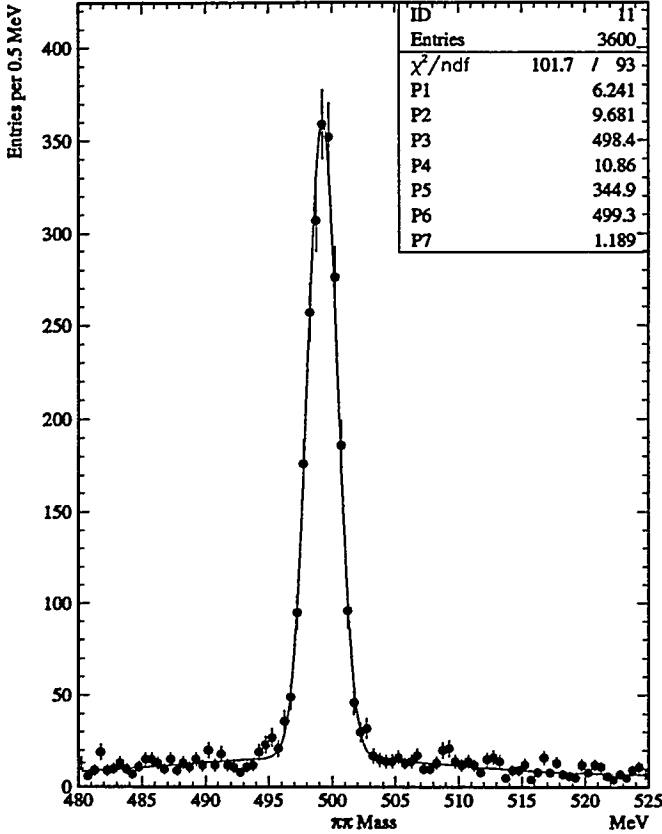


Figure 13: Preliminary results from BNL E871 show the $K_L^0 \rightarrow \pi^+\pi^-$ invariant mass distribution with resolution of about $1.2 \text{ MeV}/c^2$.

Proportional drift tubes are placed throughout the range stack providing 5% measurement resolution of the penetration range. The range of the particle, its timing, and trajectory have to be consistent with the kinematics determined from the magnetic spectrometer. The power of the background suppression comes also from kinematics: quality of reconstructed trajectories, consistency of momenta measured in two magnets, quality of the vertex, missing transverse momentum, and reconstructed invariant mass of the final-state particles.

The custom designed data acquisition system used by E871 is the same as for E791.⁴¹ Briefly, fast conversion-time front-end ADC's, TDC's, and latches are sparsely read out into dual-port memories residing in VME crates and serviced by Silicon Graphics V-35 processors. Once the memory buffer is filled with trigger events, a software algorithm reconstructing kinematics is applied. Events passing loose invariant-mass and angular requirements are retained as candidate events. Certain fraction of minimum bias events is unconditionally retained andulti-

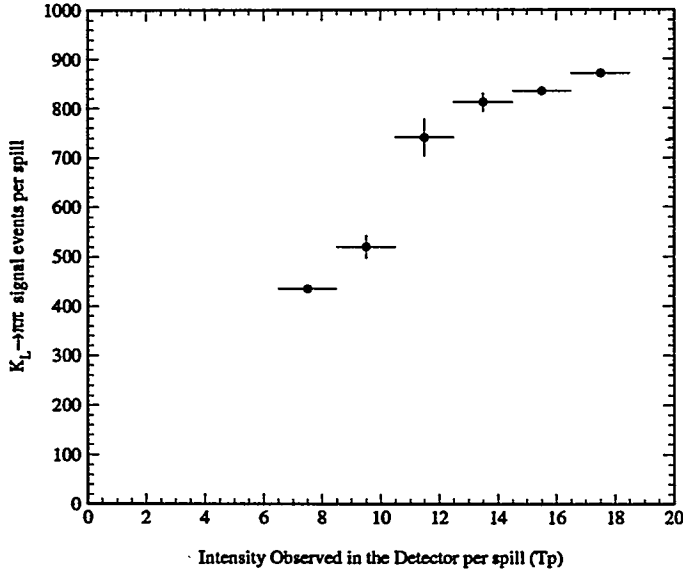


Figure 14: The number of reconstructed $K_L^0 \rightarrow \pi^+\pi^-$ events in E871 as a function of the beam intensity⁴² measured in units of Tp (1 Tp = 10^{12} protons) on target per spill. The experiment typically operates $\sim 100\%$ live at ~ 17 Tp.

mately used for the sensitivity measure of the experiment. With 17×10^{12} protons on target, there are about 750k non-parallel triggers formed by the coincidences in trigger hodoscopes. The requirement of parallelism (i.e., position correlations between scintillator slats hit in the upstream and downstream trigger banks) reduces this number to about 200k. Further position-correlated coincidences with the Cerenkov counter and/or muon hodoscopes form about 12k triggers which are read out during the AGS spill of 1.2-1.6 seconds. About 400 events per spill are retained and written to tape as either candidate events, minimum bias events, or calibration events. E871 collected data between January and mid-June of the 1995 AGS and the offline analysis is currently under way. Preliminary results, as shown in Figure 13 and 14 indicate that the apparatus operates at the expected level.⁴²

4.3 The $K^+ \rightarrow \pi^+ \mu^+ e^-$ experiment (E865)

Experiment 865^{43,44} is an upgrade of the previous experiments E777 and E851. The new spectrometer has been designed with the goal of reaching 10^{-12} single event sensitivity in the channel $K^+ \rightarrow \pi^+ \mu^+ e^-$. Observation of such a decay would explicitly demonstrate lepton-flavor violation. Due to the helicity structure of the hadronic currents, this mode is sensitive to scalar or vector interactions, while $K_L^0 \rightarrow \mu^\pm e^\mp$ process tests pseudoscalar or axial-vector forces making the two searches complementary. As argued earlier, $K^+ \rightarrow \pi^+ \mu^+ e^-$ probes mass scale of 86 TeV (eq. 5) at the 10^{-12} branching fraction.

The background to $K^+ \rightarrow \pi^+ \mu^+ e^-$ process comes primarily from $K^+ \rightarrow \pi^+ \pi^- \pi^0$ and $K^+ \rightarrow \pi^+ \pi^0$. If in the τ -decay ($K^+ \rightarrow \pi^+ \pi^- \pi^0$) one of the π^+ mesons decays in flight ($\pi \rightarrow \mu \nu_\mu$) or is misidentified as a muon, and π^- is misidentified as an electron, the observed final-state particles are π^+ , μ^+ , and e^- . Similarly, in $K^+ \rightarrow \pi^+ \pi^0$ case, if π^+ decays or is misidentified as a muon, and π^0 decays via a Dalitz mode $\pi^0 \rightarrow e^+ e^- \gamma$, and e^+ is mistaken for π^+ - this leads again to the same effective final state which mimics the real $K^+ \rightarrow \pi^+ \mu^+ e^-$. The latter source hints at the necessity to conduct the search of the $\mu^+ e^-$ and not the $\mu^- e^+$ pair. This stems from the fact that K_{e3}^+ decay ($K^+ \rightarrow \pi^0 e^+ \nu_e$) mode has a branching fraction of $B(K^+ \rightarrow \pi^0 e^+ \nu_e) = 4.82 \pm 0.06\%$ and thus is the source of positrons at a factor of ~ 20 higher level than the Dalitz source of electrons. It is worth mentioning that a search for $K^+ \rightarrow \pi^+ \mu^- e^+$ conducted in mid-1970's set an impressive 90% C.L. upper limit for this process at⁴⁵ 6.9×10^{-9} .

This charge asymmetry propagates into the detector design. Figure 15 shows the spectrometer designed and commissioned by the E865 collaboration. The key features of the apparatus are^{43,46}:

- the left arm of the spectrometer, to which negative particles are deflected by the first magnet, is optimized for an electron identification (or π^-/e^- separation);
- the right arm (with positive particles) is optimized for a muon and pion identification (or e^+/π^+ separation)
- two dipole magnets with p_T kick of $+250\text{ MeV}$ and -250 MeV provide the charge separation and a momentum measurement

E865 Apparatus
Plan Diagram

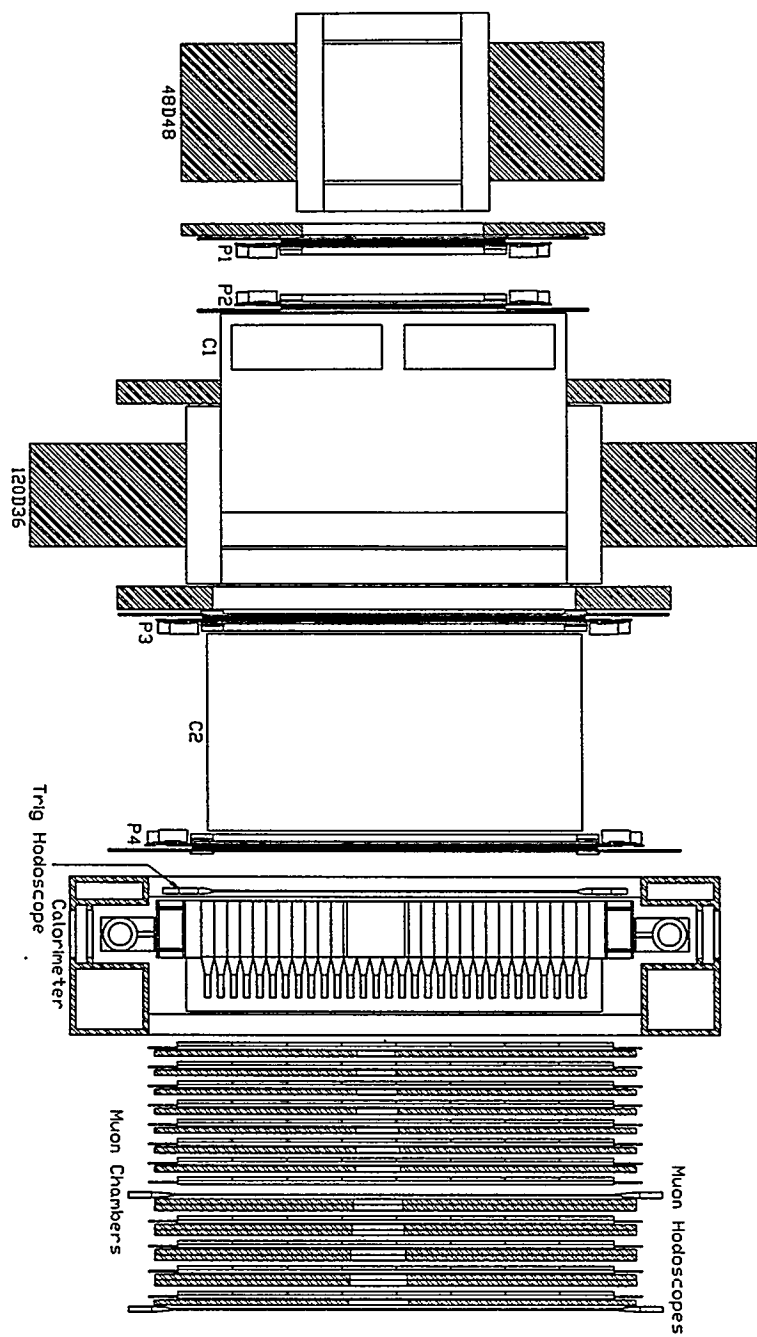


Figure 15: BNL E865 apparatus.

- redundant particle identification employs two sequential threshold Cerenkov counters, electromagnetic calorimeter, and muon range stack.

The 6 GeV/c K^+ beam was substantially upgraded for E865. It delivers kaons with about 5% momentum spread. For 1×10^{13} protons on target the flux of K^+ is about 6×10^7 , with about 2×10^9 protons and pions. K^+ decay products pass through the first dipole magnet which deflects negatively charged particles to the left, and positively charged particles to the right. A particle to be identified as an electron is required to induce signals in two left-arm hydrogen-filled Cerenkov counters. In addition, the electromagnetic calorimeter (“shishkebab” configuration of the lead-scintillator tiles with a fiber readout) should reconstruct deposited energy consistent with the momentum measured in the upstream part of the spectrometer, where particles are tracked using proportional wire chambers with resistive Mylar cathode. The right-arm particle identification is designed to discriminate against positrons. The two right-side Cerenkov counters are filled with CH_4 providing the momentum threshold for muons at 3.7 GeV, which is near the upper end of the muon momentum spectrum for $K^+ \rightarrow \pi^+ \mu^+ e^-$. Further, the electromagnetic calorimeter and muon stack with scintillation hodoscopes and proportional wire chambers provide additional discrimination. The experiment ran with about 2×10^6 three-particle trigger-counter coincidences per spill. Additional coincidences with Cerenkov counters, muon hodoscopes, and PWC’s suppressed the trigger rate to about 1000 per spill. With about 80% live-time events were read out and processed by a farm of processors which discarded events useless for further offline analysis and leaving about 50% triggers written to tape.

E865 collected data March through mid-June, 1995. In addition to lepton-flavor violation, the E865 collaboration plans to study a number of less-rare decay modes which could provide an important input (or tests) of chiral perturbation theory. These modes include $K^+ \rightarrow \pi^+ e^+ e^-$, $K^+ \rightarrow \pi^+ e^+ e^- \gamma$, $K^+ \rightarrow \pi^+ \mu^+ \mu^-$, $K^+ \rightarrow \pi^+ \gamma \gamma$, $K^+ \rightarrow \pi^+ \pi^0 e^+ e^-$, $K^+ \rightarrow e^+ e^+ e^- \nu$, and $K^+ \rightarrow \mu^+ e^+ e^- \nu$. Figure 16 shows a preliminary result of $K^+ \rightarrow \pi^+ e^+ e^-$ reconstruction from a fraction of collected data.⁴⁶

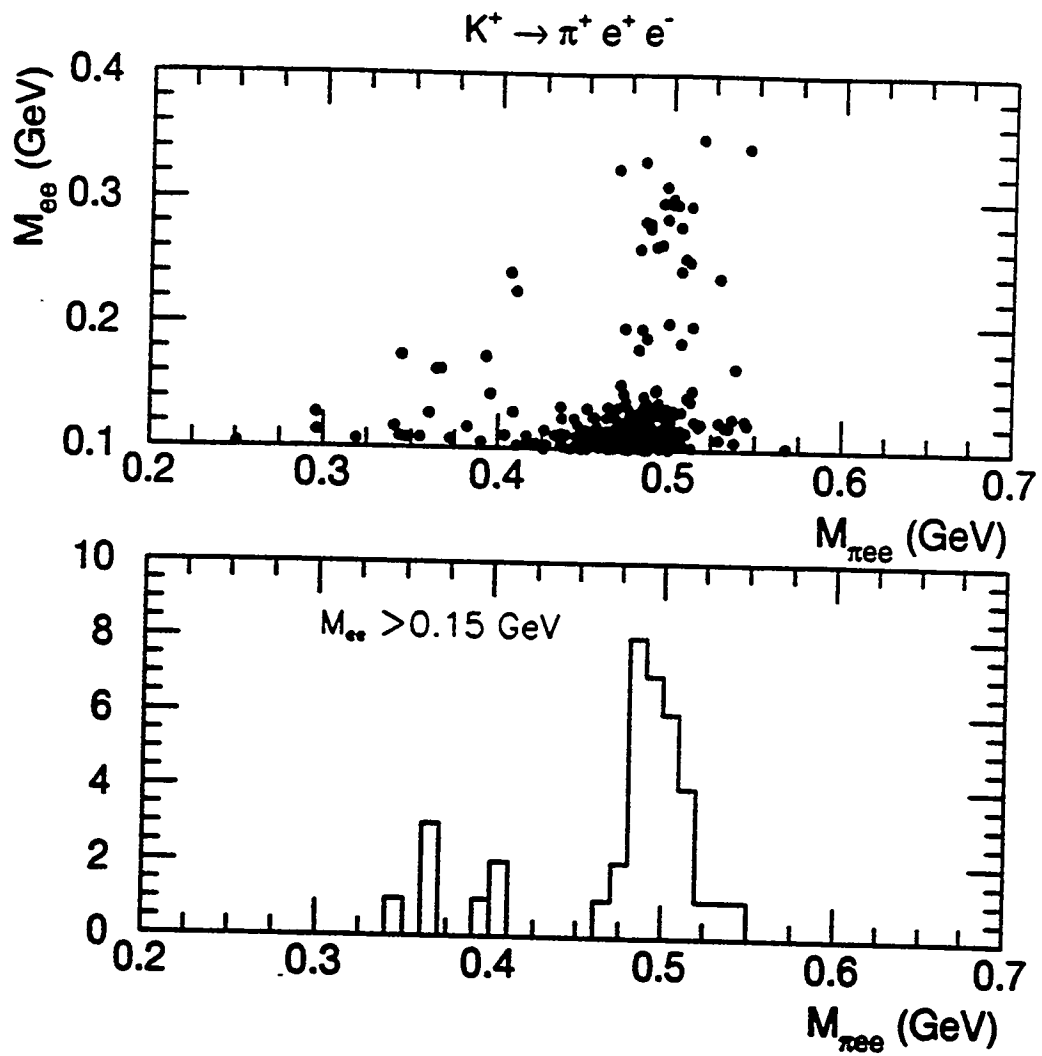


Figure 16: Preliminary results from E865: a sample of reconstructed events $K^+ \rightarrow \pi^+ e^+ e^-$ from a fraction of the collected data in 1995⁴⁶.

4.4 The $K^+ \rightarrow \pi^+ \nu \bar{\nu}$ experiment (E787)

Experiment 787⁴⁷ is a continuing effort started in the mid-1980's. The primary goal of the experiment is to make the first observation of the $K^+ \rightarrow \pi^+ \nu \bar{\nu}$ decay mode. This GIM-suppressed decay is expected at $\sim 10^{-10}$ level, but the final state presents a formidable experimental challenges. With well-understood underlying theory and a measured mass of the top quark, the observation of even a few events could be turned into a measurement of the V_{td} of the CKM matrix.

Because of the weak topological constraints the search for $K^+ \rightarrow \pi^+ \nu \bar{\nu}$ is carried with a stopping K^+ beam, and with the limited range of pion momenta above the $K^+ \rightarrow \pi^+ \pi^0$ peak. As illustrated in Figure 17, most of the $K^+ \rightarrow \pi^+ \nu \bar{\nu}$ phase-space lies below the $K^+ \rightarrow \pi^+ \pi^0$ momentum peak of 205 MeV/c, but the severe background due to π^+ from $K^+ \rightarrow \pi^+ \pi^0$ (π^+ can interact with the detector material and shift down its energy) makes this region experimentally difficult at low sensitivities. The main background above the $K^+ \rightarrow \pi^+ \pi^0$ peak is due to misidentified muons from $K^+ \rightarrow \mu^+ \nu_\mu$ and $K^+ \rightarrow \mu^+ \nu_\mu \gamma$, as well as from mismeasured π^+ 's from $K^+ \rightarrow \pi^+ \pi^0$ if the two photons from π^0 are missed. In addition, pions in the beam can be mistaken for kaons. Also misidentified muons and/or protons originating from $K^+ n \rightarrow K^0 p$ and followed by $K^0_L \rightarrow \mu \nu$ pose a background threat.

The experimental approach undertaken by the E787 collaboration emphasizes⁴⁸:

- redundant determination of the pion kinematics by independent measurements of pion's momentum, kinetic energy, range, and dE/dx
- observation and measurement of timing and range relationships of the $\pi \rightarrow \mu \rightarrow e$ decay sequence
- nearly 4π solid-angle photon hermeticity of the apparatus

The present E787 apparatus is shown in Figure 18. This is an upgraded version of the spectrometer used in 1989-1991.⁴⁹ Two electrostatic separators are used to deliver 800 MeV/c K^+ 's. The beam provides three times more kaons than pions. Kaons are identified by Cerenkov and dE/dx counters placed in the beam. Passing the BeO degrader kaons are stopped in an active target made of scintillation fibers located in the center of the apparatus. The target is surrounded by the central drift chamber covering about 2π solid-angle and used to determine momenta of particles

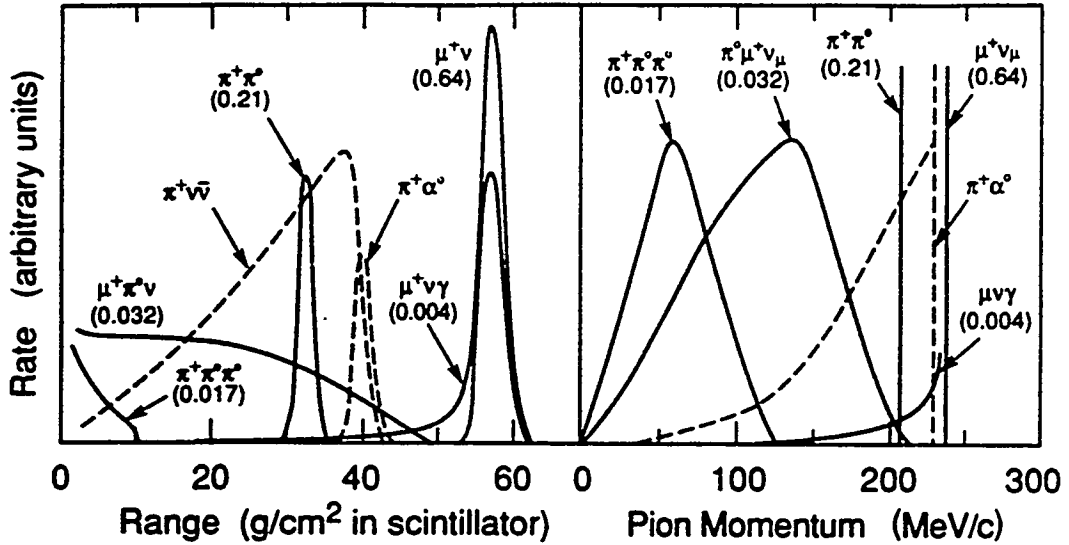


Figure 17: Range and momentum spectra of π^+ from $K^+ \rightarrow \pi^+ \nu \bar{\nu}$ and from the major sources of backgrounds.

through trajectory curvature in 1 T solenoidal magnetic field in the apparatus. Further, in the central (barrel) part of the apparatus a scintillator range stack is used to provide kinetic energy and range measurement of pions. In addition, pions are distinguished from muons by identifying $\pi \rightarrow \mu \rightarrow e$ decay sequence using 500-MHz transient digitizers. Finally, photon detectors (lead-scintillator stack in the barrel part, and CsI blocks in the endcap) assure hermeticity to photons.

The thickness of the stack is optimized to catch pions with momentum $214 \leq P_\pi \leq 231$ MeV/c and range $34 \leq R_\pi \leq 40$ cm in scintillator, and to achieve ~ 1 cm range resolution. Additional constraints on tagging of transitions $\pi^+ \rightarrow \mu^+$ and $\mu^+ \rightarrow e^+$ in transient digitizers, beam and photon vetoing bring an overall acceptance for $K^+ \rightarrow \pi^+ \nu \bar{\nu}$ to only few % level. E787 took data with an upgraded apparatus between January and mid-June, 1995. The beam provided about 1.3 million stopping K^+ 's per spill. A multi-level trigger reduced this number to about couple of hundred events which were written to tape. Figure 19 shows an example of improvement in timing and energy resolutions achieved in 1995 data. Besides the $K^+ \rightarrow \pi^+ \nu \bar{\nu}$ mode the collaboration will also study several other topologically and kinematically related kaon decay modes. For example,

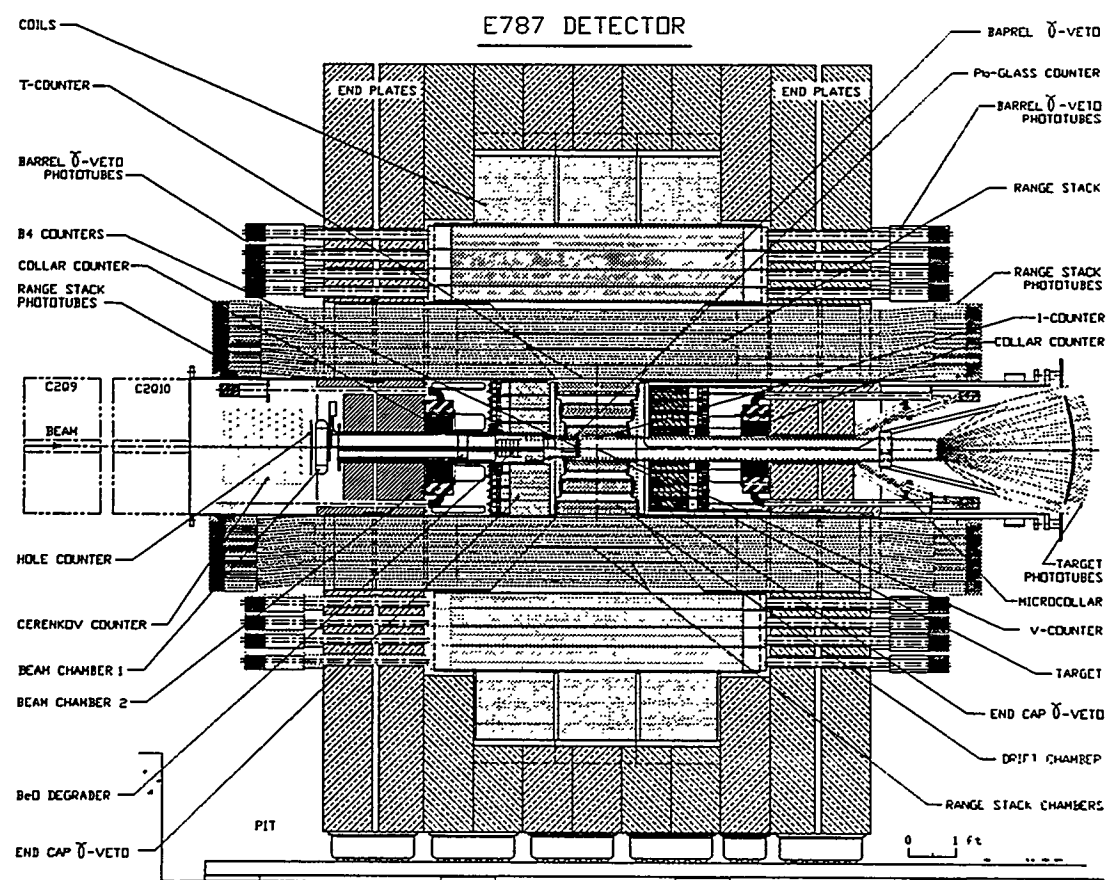
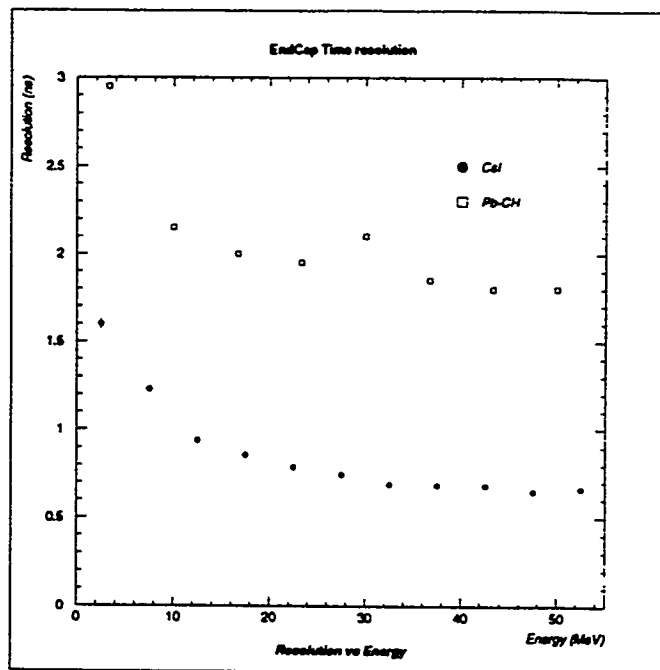
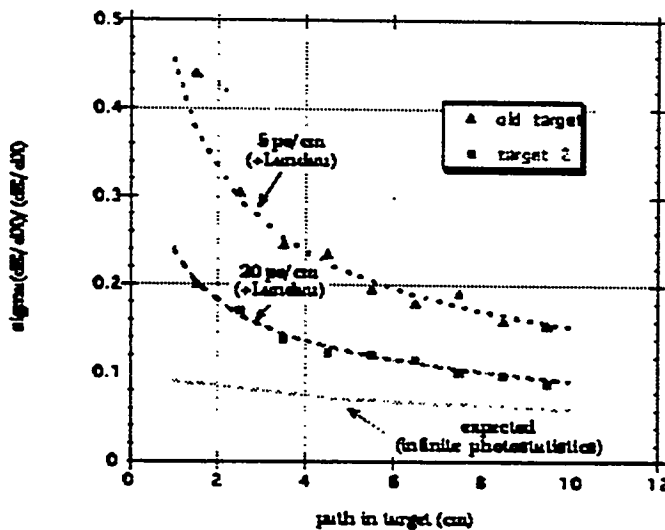


Figure 18: BNL E787 apparatus.



(a)



(b)

Figure 19: Improvements of the upgraded E787 apparatus as determined from the 1995 data⁴⁸: (a) improved photon timing of the newly installed CsI blocks (circles) versus old lead-scintillator stack(squares); (b) improved energy resolutions.

Decay mode	Projected Sensitivity	Experiment
$K_L^0 \rightarrow \mu^\pm e^\mp$	$\sim 1 \times 10^{-12}$	E871
$K_L^0 \rightarrow e^+ e^-$	$\sim 1 \times 10^{-12}$	
$K_L^0 \rightarrow \mu^+ \mu^-$	several thousands events	
$K^+ \rightarrow \pi^+ \mu^+ e^-$	$\sim 1 \times 10^{-12}$	E865
$K^+ \rightarrow \pi^+ \nu \bar{\nu}$	$\sim 1 \times 10^{-10}$	E787

Table 4: Projected sensitivities of the three experiments at the AGS.

$K^+ \rightarrow \pi^+ X^0$ would give similar signature to $K^+ \rightarrow \pi^+ \nu \bar{\nu}$ if X^0 is a weakly interacting (new) particle. Motivated by their significance in chiral perturbation theory, and the fact that they are experimentally accessible at the same time as $K^+ \rightarrow \pi^+ \nu \bar{\nu}$ decays, channels like $K^+ \rightarrow \pi^+ \mu^+ \mu^-$, $K^+ \rightarrow \pi^+ \pi^0 \gamma$, $K^+ \rightarrow \pi^+ \gamma \gamma$, $K^+ \rightarrow \mu^+ \nu_\mu \gamma$, and $K^+ \rightarrow \pi^0 \mu^+ \nu_\mu \gamma$ will be studied.

5 Summary and Conclusions

We have presented a brief summary of best results and described current experiments at the AGS at BNL in the area of very rare kaon decays. This active program, which was started in the early 1980's, has brought a major advancement in testing "rare physics" within the Standard Model and in searching for processes outside of it. The current round of experiments will probe mass scales unattainable in direct searches, and will possibly observe the lowest particle decay branching fraction of any kind. Table 4 summarizes sensitivities expected for the main rare decay modes studied by the three collaborations at BNL.

For the currently scheduled running experiment 871 should be able to reach 10^{-12} single event sensitivity in $K_L^0 \rightarrow \mu^\pm e^\mp$, probing ~ 200 TeV mass scale for the new interactions. Reaching low branching ratios will allow to collect several thousand of $K_L^0 \rightarrow \mu^+ \mu^-$ events and substantially improve the branching ratio measurement. In addition, the first observation of $K_L^0 \rightarrow e^+ e^-$ expected at $\sim 3 \times 10^{-12}$ should be possible. Complementarily, the near future of the experiment 865 should bring ability to probe ~ 80 TeV mass range in $K^+ \rightarrow \pi^+ \mu^+ e^-$ and study other decays to test and expand reliability of chiral perturbation theory. With improved capabilities the collaboration is considering also studying CP

asymmetries in $K^+ \rightarrow \pi^+ \pi^- \pi^0$. Experiment 787 plans a continuing program of upgrades and expects ultimately to measure the $B(K^+ \rightarrow \pi^+ \nu \bar{\nu})$ with 20% uncertainty. This will be an important test of the Standard Model and will provide an important input to determining the $V_{ts}^* V_{td}$ quantity of the CKM matrix, shedding more light onto the current picture of the CP violation.

I would like to thank L. Littenberg and M. Zeller for providing useful information, and J. Ritchie for comments on the manuscript.

References

- [1] H. Haber and G. L. Kane, Phys. Rep. **117**, 75(1985); B. A. Campbell, Phys. Rev. **D28**, 209(1983); J. C. Romao *et al.*, Nucl. Phys. **B250**, 295(1985).
- [2] E. Farhi and L. Susskind, Phys. Rep. **74**, 277(1981); E. Eichten and K. Lane, Phys. Lett. **90B**, 125(1980); J. Ellis *et al.*, Nucl. Phys. **B182**, 529(1981); A. Masiero, E. Papantonopoulos, and T. Yanagida, Phys. Lett. **115B**, 229(1982); B. Holdom, Phys. Lett. **143B**, 227(1984); E. Eichten *et al.*, Phys. Rev. **D34**, 1547(1986).
- [3] J. C. Pati and A. Salam, Phys. Rev. **D10**, 275(1974); A. Barroso, G. C. Branco, and M. C. Bento, Phys. Lett. **134B**, 123(1984).
- [4] T. Maehara and T. Yanagida, Prog. Theo. Phys. **60**, 1434(1979); A. Davidson and K. C. Wali, Phys. Rev. Lett. **26**, 691(1981); Wei-Shu Hou and A. Soni, Phys. Rev. Lett. **54**, 2083(1985).
- [5] Z. Y. Zhu, Z. Phys. **C13**, 321(1982); I. Bars, M. J. Bowick, and K. Freese, Phys. Lett. **138B**, 159(1984); O. W. Greenberg, R. N. Mohapatra, and S. Nussinov, Phys. Lett. **148B**, 465(1984); J. C. Pati, Phys. Rev. **D30**, 1144(1984).
- [6] B. A. Campbell *et al.*, Int. J. Mod. Phys. **A2**, 831(1987).
- [7] Rare K Decays, J. L. Ritchie and S. G. Wojcicki, Rev. Mod. Phys. **65**, 1149(1993); Rare and Radiative Kaon Decays, L. Littenberg and G. Valencia, Ann. Rev. Nucl. Part. Sci. **43**, 729(1993); The Search for Direct CP Violation, B. Winsstein and L. Wolfenstein, Rev. Mod. Phys. **65**, 1113(1993);
- [8] A. J. Buras, Preprint MPI-PhT/95-30, April, 1995.

- [9] L. M. Sehgal, Preprint PITHA 94/52, November, 1994; to appear in Proceedings of The Third Workshop on High Energy Particle Physics, Madras, Jan. 10-22, 1994.
- [10] N. Bilic and B. Guberina, *Fortsch. Phys.* **42**,209(1994).
- [11] R. N. Cahn and H. Harari, *Nucl. Phys.* **B176**,135(1980).
- [12] D. Rein and L. M. Sehgal, *Phys. Rev.* **D39**,3325(1989); M. Lu and M. B. Wise, *Phys. Lett.* **B324**,461(1994).
- [13] J. Hagelin and L. Littenberg, *Prog. Part. Nucl. Phys.* **23**,1(1989).
- [14] I. Bigi and F. Gabbiani, *Nucl. Phys.* **B367**,3(1991).
- [15] G. Buchalla, A. Buras, and M. Harlander, *Nucl. Phys.* **B349**,1(1991)
- [16] G. Buchalla, A. Buras, and M. Harlander, *Nucl. Phys.* **B412**,106(1994)
- [17] S. Glashow, J. Iliopoulos, L. Maiani, *Phys. Rev.* **D2**,1285(1970).
- [18] L. M. Sehgal, *Phys. Rev.* **183**,1511(1969). *Nuovo Cimento* **45**,785(1966).
- [19] Review of Particle Properties, *Phys. Rev.* **D50**,1173-1826(1994).
- [20] A. Buras and M. Harlander, in "Heavy Flavours", edited by A. Buras and M. Lindner, (World Scientific 1992), p. 58.
- [21] T. Inami and C. S. Lim, *Prog. Theor. Phys.* **65**,297(1981), Erratum 1772.
- [22] G. Belanger and C. Q. Geng, *Phys. Rev.* **D43**,140(1991).
- [23] P. Ko, *Phys. Rev.* **D45**,174(1992).
- [24] K. Arisaka *et al.*, *Phys. Rev. Let.* **70**,1049(1993).
- [25] T. Akagi *et al.*, *Phys. Rev. Let.* **67**,2614(1991).
- [26] S. F. Schaffner *et al.*, *Phys. Rev.* **D39**,990(1989)
- [27] A. M. Lee *et al.*, *Phys. Rev. Let.* **64**,165(1990).
- [28] S. Adler *et al.*, BNL-62327, PRINCETON/HEP/95-8, TRI-PP-95-83.
- [29] A. P. Heinson *et al.*, *Phys. Rev.* **D51**,985(1995).
- [30] T. Akagi *et al.*, *Phys. Rev. Let.* **67**,2618(1991).
- [31] K. Arisaka *et al.*, *Phys. Rev. Let.* **71**,3910(1993).
- [32] E. Jastrzembski *et al.*, *Phys. Rev. Lett.* **61**,2300(1988)
- [33] C. Alliegro *et al.*, *Phys. Rev. Let.* **68**,278(1992).

- [34] M. S. Atiya *et al.*, Phys. Rev. Let. **70**,2521(1993).
- [35] M. S. Atiya *et al.*, Phys. Rev. Let. **63**,2177(1989).
- [36] A. Deshpande *et al.*, Phys. Rev. Let. **71**,27(1993).
- [37] K. S. McFarland *et al.*, Phys. Rev. Let. **71**,31(1993).
- [38] A. Heinson *et al.*, AGS Proposal 871, September 1990.
- [39] E871 is a collaboration of: *The University of California at Irvine* - M. Bachman, D. Connor, P. deCecco, N. Kanematsu, R. Lee, W. Molzon; *Stanford University* - K. Ecklund, K. Hartman, M. Hebert, G. Irwin, D. Ouimette, M. Pommot-Maia, S. Wojcicki; *The University of Texas at Austin* - D. Ambrose, S. Graessle, M. Hamela, G. Hoffmann, K. Lang, J. McDonough, A. Milder, P. Riley, J. Ritchie, V. Vassilakopoulos, B. Ware, S. Worm; *College of William & Mary* - M. Eckause, D. Hancock, C. Hoff, J. Kane, Y. Kuang, R. Martin, R. Welsh, E. Wolin; *University of Richmond* - P. Rubin.
- [40] S. Worm, Ph. D. Thesis, University of Texas, Austin, June, 1995.
- [41] R. D. Cousins *et al.*, Nucl. Instr. Meth. **A277**,517(1989).
- [42] M. Hebert, talk presented at the AGS Users Meeting, BNL, June 15, 1995.
- [43] AGS Proposal 865, May 1990.
- [44] E865 is a collaboration of: *Brookhaven National Laboratory* - D. Lazarus, L. Leipuner, H. Ma, P. Rehak; *Institute for Nuclear Research, Moscow* - G. S. Atoyan, V. V. Isakov, A. A. Poblaguyev, V. Postoev, A. Proskurjakov; *Joint Institute for Nuclear Research, Dubna* - B. Z. Zalikhanov; *University of New Mexico* - B. Bassalleck, S. Eilerts, H. Fisher, J. Lowe, D. Wolfe; *Paul Scherrer Institute* - W. Djordjadze, J. Egger, W. D. Herold, H. Kaspar, J. Missimer; *University of Basel* - G. Backendstoss, W. Menzel, H. Weyer; *University of Pittsburgh* - V. Atoyan, K. Baker (Hampton Univ.), E. Battiste, M. Gach, C. Felder, D. E. Krauss, M. Shubin, J. A. Thompson; *High Energy Physics Institute, Tbilisi State University* - N. Amaglobeli, Y. Bagaturia, D. Mazavia, T. Sachelashvili; *Yale University* - R. Appel, D. Bergman, S. Dhawan, H. Do, J. Lozano (Univ. of Connecticut), M. Zeller; *University of Zurich* - S. Pislak, P. Truoel.
- [45] A. M. Diamant-Berger *et al.*, Phys. Lett. **B62**,485(1976).
- [46] H. Ma, talk presented at the AGS Users Meeting, BNL, June 15, 1995.

[47] E787 is a collaboration of: *Brookhaven National Laboratory* - S. Adler, M.S. Atiya, I-H. Chiang, M. Diwan, J.S. Frank, J.S. Haggerty, S.H. Kettell, T.F. Kycia, K.K. Li, L.S. Littenberg, A.J. Stevens, R.C. Strand, C.H. Witzig; *INS, University of Tokyo* - K. Ino, T. Komatsubara, N. Muramatsu, H. Okuno, S. Sugimoto, K. Ukai; *KEK, National Laboratory for High Energy Physics* - T. Inagaki, S. Kabe, M. Kobayashi, Y. Kuno, T. Sato, T. Shinkawa, Y. Yoshimura; *Osaka University* - Y., Kishi, T. Nakano; *Princeton University* - M. Ardebili, M. Convery, M.M. Ito, D.R. Marlow, R. McPherson, P.D. Meyers, F.C. Shoemaker, A.J.S. Smith, B. Stone; *TRIUMF* - M. Aoki, E.W. Blackmore, D.A. Bryman, P. Kitching, A. Konaka, J.A. Macdonald, J. Mildenberger, T. Numao, J-M. Poutissou, R. Poutissou, G. Redlinger, J. Roy, M. Rozon, R. Soluk, A.S. Turcot.

[48] G. Redlinger, talk presented at the AGS Users Meeting, BNL, June 15, 1995; T. K. Komatsubara, talk presented at the AGS Users Meeting, BNL, June 15, 1995.

[49] M. S. Atiya *et al.*, Nucl. Instr. Meth. **A321**, 129 (1992).

